

# Entropic and algebraic transcript-based tools in time series analysis

José M. Amigó<sup>1</sup> and Roberto Dale<sup>1</sup>

*Centro de Investigación Operativa, Universidad Miguel Hernández, 03202 Elche, Spain*

(\*Electronic mail: jm.amigo@umh.es, rdale@umh.es.)

(Dated: 29 May 2026)

Algebraic representations of time series are symbolic representations whose symbols belong to a finite group. Precisely, the framework of the present paper is the analysis of coupled time series in algebraic representations and, more generally, group-valued time series. The prototype of an algebraic representation is an ordinal representation, whose symbols are permutations, also called ordinal patterns in the context of time series analysis. In fact, permutations, endowed with function composition, build a group called a symmetric group. A simple way to harness the algebraic structure of the alphabet in such cases is the concept of transcript from one group element to another. Since transcripts involve two group elements, they are very suitable for studying couplings between time series in the same algebraic representation. In this paper, we outline several existing entropic and algebraic transcript-based tools for analyzing coupled time series and systems. In addition to entropy, the entropic tools include divergence, statistical complexity and mutual information. The algebraic tools comprise order classes and, most recently, the Cayley and Kendall distances. We use the detection of generalized synchronization in a well-studied coupled system to compare the performances of some of those tools. To this end, we also provide an alternative tool called the similarity distance between time series, which is a mean Kendall distance. We found that the novel similarity distance outperforms the other tools tested.

**Symbolization is a useful method to gain valuable insights in time series analysis. To do this, the entries are generally discretized and replaced with symbols. In the case of algebraic representations (one of the main characters of this paper), the symbols make up an algebraic structure called a group, which allows for additional leverage. Such is the case when the symbols are permutations (also called ordinal patterns), obtained by ranking the entries of a time series within sliding windows. This symbolization technique has become very popular among data analysts not only for its conceptual simplicity and practical advantages, but also for its proven power in extracting useful information from data. A simple way to exploit the algebraic properties of the symbols in algebraic representations is the concept of transcript. In this paper, we discuss the basics of transcripts, their connection with two algebraic distances in both permutation and general groups, and the application of transcript-based tools in the analysis of coupled time series.**

## I. INTRODUCTION

Symbolic representation of time series is a usual technique in time series analysis<sup>1</sup>, where by time series we mean here finite or infinite sequences of real numbers (the data). The perhaps simplest instance consists of partitioning the range of the data and labeling the resulting intervals; the entries of the time series are then trade-off for the labels of the intervals they belong to. This procedure is well known in statistics and dynamical systems<sup>2</sup>. More general methods trade-off segments of the time series (even the whole series if finite) for graphs, topological properties or algebraic structures, such as different types of networks<sup>3-5</sup>, topological invariants<sup>6-8</sup> and finite groups<sup>9</sup>. In such cases, we speak of graph-theoretical, topological and algebraic representations, respectively. The pro-

toype of the latter are the ordinal representations, i.e., symbolic representations whose symbols are rank vectors, usually referred to as ordinal patterns<sup>10,11</sup> in time series analysis. Therefore, ordinal patterns can be viewed as permutations, which build a classic algebraic group called the symmetric group<sup>12,13</sup>.

In this paper we are going to focus on algebraic representations and how to take advantage of the fact that their alphabets are groups. To the best of our knowledge, the algebraic nature of ordinal patterns was first exploited by Monetti et al.<sup>14</sup>, who introduced the concept of transcript from one ordinal pattern to another; its generalization to algebraic representations is straightforward<sup>9</sup>. Furthermore, since transcripts involve two symbols, they are well-suited for studying serial dependence in time series (self-transcripts) and the coupling between systems (cross-transcripts)<sup>15</sup>. We are not aware of any other proposals in this regard.

Therefore, here we will discuss the concept of transcript in a group, present some traditional, recent and novel transcript-based tools in time series analysis, and illustrate their applications with numerical simulations. Among the traditional tools, we consider some entropic ones (basically: entropy, divergence and mutual information) and the algebraic order classes, all of which have a record of practical applications<sup>14,15</sup>. The recent tools comprise two algebraic distances, namely, the Cayley and Kendall distances<sup>16</sup>. And the novel tool is a mean Kendall distance between two time series proposed in this paper, which we call the similarity distance.

To compare the performance of the above-mentioned transcript-based tools, we use the detection of generalized synchronization in a drive-response system. As it turns out, the performance of the similarity distance compares favorably with that of the entropy-complexity plane, transcript mutual information, transcript order classes, and the transcript probability distribution-based Jensen-Shannon distance (the square root of the Jensen-Shannon divergence). This suggests that the similarity distance can be a useful tool in time series analysis.

Interestingly, as we transition from the concept of transcript to its applications in time series analysis, we will come across direct connections between transcripts and basic results in group theory, a very rewarding fact because transcripts are a hallmark of algebraic representations. Indeed, the transcript from one group element to another can be used to calculate the Cayley and Kendall distances between them. Moreover, Cayley's theorem, which embeds any finite group into a certain symmetric group, can be implemented via transcripts. Incidentally, Cayley's embedding shows that ordinal patterns are a kind of universal symbols for algebraic representations, although this encoding is practical only for small groups<sup>16</sup>.

To sum up, this paper has three main objectives.

- (1) To provide an overview of transcripts and their applications in algebraic representations of time series;
- (2) To compare the performances of several transcript-based tools using numerical simulations;
- (3) To present a novel algebraic tool, the similarity distance (a mean Kendall distance), which outperforms the other options in our numerical tests.

With these objectives in mind, this paper is organized as follows. We begin by introducing the main characters: permutation groups (Section II), algebraic representations of time series (Section III), and the concept of transcript (Section IV). The latter will then allow us to implement a homomorphism from any finite group to a group of permutations (Cayley's theorem). In Section V we outline a selection of entropic and algebraic transcript-based tools for time series analysis. This selection ranges from the more traditional ones (entropy, entropy-like quantities and order classes) to the more recent ones (the Cayley and Kendall distances). The numerical simulations of Section VI using two non-identical, unidirectionally coupled Hénon maps aim to illustrate the potential of the afore-mentioned tools in applications, in this case, for detecting generalized synchronization. One of these tools is the similarity distance, proposed in Section VID, which discriminates between strong and weak generalized synchronizations better than its competitors. The conclusions, together with a summary of the main contributions of this paper, are the content of Section VII.

## II. ORDINAL REPRESENTATIONS AND THE GROUPS OF PERMUTATIONS

The concept of algebraic representation in time series analysis is central to this article. In this section we present its prototype, the ordinal representation, a symbolic representation of time series whose symbols are permutations, also called ordinal patterns, which was proposed by Bandt and Pompe<sup>10</sup>.

Let  $x = (x_t)_{t \geq 0}$  be an  $\mathbb{R}$ -valued time series. The *ordinal representation* of  $x$  with parameter  $L \geq 2$  is the symbolic time series  $(\mathbf{r}_t)_{t \geq 0}$ , where  $\mathbf{r}_t = (r_1, r_2, \dots, r_L)$  is the rank vector of the sequence (window, block, word, ...)  $x_t^L := x_t, x_{t+1}, \dots, x_{t+L-1}$ , i.e.,

$$x_{t+r_1-1} < x_{t+r_2-1} < \dots < x_{t+r_L-1}. \quad (1)$$

We will write  $\mathbf{r}_t = \text{rank}(x_t^L)$  and use the set  $\{1, 2, \dots, L\}$  to rank the elements of  $x_t^L$ . For example, if  $x_t^3 = 1.7, 0.5, 1.2$ , then  $\mathbf{r}_t = (2, 3, 1)$ . In case of a tie  $x_{t+i} = x_{t+j}$ , there are several conventions, e.g.,  $x_{t+i} < x_{t+j}$  if  $i < j$ . The perhaps most popular convention (especially if there are many ties) is to add random noise to eliminate the tie<sup>17</sup>. In addition to equation (1), other definitions of ordinal patterns can be found in the literature<sup>18–20</sup>.

In equation (1) it is assumed that the delay time  $T$  used to analyze the time series  $x$  is 1. In practice, though, when the rate of change of the data is small compared to the sampling frequency of the signal, it may be convenient to use  $T > 1$ , in which case equation (1) generalizes to

$$x_{t+r_1 T-1} < x_{t+r_2 T-1} < \dots < x_{t+r_L T-1}. \quad (2)$$

Therefore, ordinal representations have two parameters: the length of the patterns  $L \geq 2$  (sometimes called embedding dimension) and the delay time  $T \geq 1$  (also called delay lag). Here  $T = 1$ , unless otherwise stated. An overview of selection techniques for delay times can be found in Tan et al.<sup>21</sup>.

The rank vectors  $\mathbf{r}_t = \text{rank}(x_t^L)$  are usually called *ordinal patterns* of length  $L$ , ordinal  $L$ -patterns, or simply  $L$ -patterns if the only patterns in question are the ordinal ones. They are also aptly called permutations since, as any total ranking,  $\mathbf{r}_t = (r_1, r_2, \dots, r_L)$  can be viewed as the one-line form of the permutation

$$\begin{pmatrix} 1 & \dots & k & \dots & L \\ r_1 & \dots & r_k & \dots & r_L \end{pmatrix}. \quad (3)$$

This is the view that best suits our purposes. For this reason, we will mainly use the one-line form  $(r_1, r_2, \dots, r_L)$  and only occasionally the two-line form (3) for permutations. In numerical examples, the permutation  $(r_1, r_2, \dots, r_L)$  will be shortened to  $r_1 r_2 \dots r_L$ ; for example, the permutation  $(2, 3, 1)$  will be written as 231.

**Remark 1** *Other symbols for the rank relationships (1) and (2) have also been used in the literature, e.g., 0-1 square matrices by Bunk et al.<sup>22</sup> and Haruna<sup>23</sup>, antisymmetric matrices with off-diagonal components  $\pm 1$  by Rios de Souza and Hlinka<sup>24</sup>, and the so-called "rank sequences" by Haruna and Nakajima<sup>25</sup>.*

Ordinal patterns have been used for classification<sup>26,27</sup>, characterization of dynamics and couplings<sup>10,14,28</sup>, tests of serial dependence<sup>29–31</sup>, and even cryptanalysis<sup>32</sup>. A generalization of ordinal patterns to multivariate data was proposed by Mohr et al.<sup>11</sup>.

Regarding the objectives of this paper, the most important feature of the ordinal representation  $(\mathbf{r}_t)_{t \geq 0}$  is the fact that the symbols  $\mathbf{r}_t$  belong to a group. In general, a group  $(\mathcal{G}, \cdot)$  is a set  $\mathcal{G}$  endowed with a binary operation " $\cdot$ ", sometimes called composition law or product, satisfying the following properties<sup>13,33</sup>.

**(G1): Associativity:** For all  $a, b, c \in \mathcal{G}$ , it is true that  $(a \cdot b) \cdot c = a \cdot (b \cdot c)$ .

**(G2): Identity element:** There exists an element  $e \in \mathcal{G}$ , called the *unity* (or *neutral*) *element*, such that  $a \cdot e = e \cdot a = a$  for all  $a \in \mathcal{G}$ .

**(G3): Inverse element:** For every  $a \in \mathcal{G}$ , there exists an element  $a^{-1} \in \mathcal{G}$ , called the *inverse element* of  $a$ , such that  $a \cdot a^{-1} = a^{-1} \cdot a = e$ .

It can be proved that the identity of a group and the inverse of each element are unique. Groups whose product is commutative (i.e.,  $a \cdot b = b \cdot a$  for all  $a, b \in \mathcal{G}$ ) are called *commutative* or *abelian*. Examples of abelian groups are the real numbers endowed with addition, and the nonzero real numbers endowed with multiplication; examples of non-commutative groups will appear shortly. If the product is clear from the context, then  $(\mathcal{G}, \cdot)$  is shortened to  $\mathcal{G}$ .

In the case of the *ordinal representation* with parameter  $L$ , the representation group is the *symmetric group of degree  $L$* , denoted  $\text{Sym}(S)$ , where  $\text{Sym}(S)$  is composed of the permutations (i.e., bijections) of a set  $S$  with cardinality  $|S| = L$  and the binary operation is the composition of permutations. Since the properties of  $\text{Sym}(S)$  do not depend on  $S$  but only on  $|S|$ , we choose the conventional set  $S = \{1, 2, \dots, L\}$  (see equation (3)), unless otherwise stated, and also denote  $\text{Sym}(S)$  by  $\text{Sym}(|S|)$  or  $\text{Sym}(L)$ . The basic properties of  $\text{Sym}(L)$  are: (i) its identity element is the identity permutation  $\text{id} = (1, 2, \dots, L)$ , (ii) it is non-commutative for  $L \geq 3$ , and (iii) its cardinality is  $L!$ .

At this point, it is important to make a note on the composition of permutations (and functions for that matter). There are two ways to define the composition  $\mathbf{r} \cdot \mathbf{s}$  of two permutations  $\mathbf{r}, \mathbf{s} \in \text{Sym}(S)$ . In the conventional definition (as a “left action” of the group on itself<sup>16</sup>),  $(\mathbf{r} \cdot \mathbf{s})(k) := \mathbf{r}(\mathbf{s}(k)) \equiv (\mathbf{r} \circ \mathbf{s})(k)$  for all  $k \in S$ , where “ $\circ$ ” stands for the composition of functions. In this case, the second permutation  $\mathbf{s}$  acts first and the first permutation  $\mathbf{r}$  acts second, so that

$$\mathbf{r} \circ \mathbf{s} = (r_1, r_2, \dots, r_L) \circ (s_1, s_2, \dots, s_L) = (r_{s_1}, r_{s_2}, \dots, r_{s_L}). \quad (4)$$

However, it is more natural in calculations that  $\mathbf{r}$  acts first and then  $\mathbf{s}$ , in which case one speaks of a “right action” of the group on itself<sup>16</sup>. Formally, one writes then  $(k)(\mathbf{r} \cdot \mathbf{s}) := ((k)\mathbf{r})\mathbf{s} \equiv (\mathbf{r} * \mathbf{s})(k)$  for all  $k \in S$ , i.e.,

$$\mathbf{r} * \mathbf{s} = (r_1, r_2, \dots, r_L) * (s_1, s_2, \dots, s_L) = (s_{r_1}, s_{r_2}, \dots, s_{r_L}). \quad (5)$$

Note that

$$\mathbf{r} * \mathbf{s} = \mathbf{s} \circ \mathbf{r}. \quad (6)$$

In this paper, we will use the definition (5) because this is the usual choice in the literature, particularly in papers dealing with transcripts. See Amigó and Dale<sup>16</sup> for a brief overview on group actions where, however, the conventional composition (4) is chosen; use equation (6) to switch between both definitions. For mathematical accounts, the interested reader is referred to the books by Lang<sup>13</sup> and Fraleigh<sup>33</sup>.

**Example 2** For further references, the multiplication table of  $(\text{Sym}(3), *)$ , the most common group in ordinal

representations<sup>34,35</sup>, is

$\mathbf{r} * \mathbf{s}$	123	132	213	231	312	321
123	123	132	213	231	312	321
132	132	123	231	213	321	312
213	213	312	123	321	132	231
231	231	321	132	312	123	213
312	312	213	321	123	231	132
321	321	231	312	132	213	123

where the composition  $\mathbf{r} * \mathbf{s}$  is calculated as in equation (5),  $\mathbf{r}$  labels the rows (leftmost column) and  $\mathbf{s}$  labels the columns (topmost row). The six permutations of  $\text{Sym}(3)$  are ordered lexicographically.

### III. ALGEBRAIC REPRESENTATIONS

In this section we generalize the ordinal representation of time series discussed in Section II. To this end, we consider symbolic representations  $\alpha = (\alpha_t)_{t \geq 0}$  of real-valued time series  $x = (x_t)_{t \geq 0}$  whose alphabet is now a general group.

To begin with, discretization of a real-valued time series  $x = (x_t)_{t \geq 0}$  produces a discrete-valued random sequence, both if  $x$  is a random trajectory and a (in general, projection of a higher dimensional) deterministic orbit, as assumed in non-linear time series analysis.

To be more specific, let  $x = (x_t)_{t \geq 0}$  be the orbit of the initial condition  $x_0$  generated by a measure-preserving dynamical system  $(\Omega, \mathcal{B}, \mu, f)$ , i.e., (i)  $(\Omega, \mathcal{B}, \mu)$  is a probability space (where  $\Omega$  is the state space of the system,  $\mathcal{B}$  is a sigma-algebra of subsets of  $\Omega$ , and  $\mu$  is a positive measure on the measurable space  $(\Omega, \mathcal{B})$ ), (ii)  $f : \Omega \rightarrow \Omega$  is a measurable mapping preserving the measure  $\mu$  (that is,  $\mu(f^{-1}(B)) = \mu(B)$  for all  $B \in \mathcal{B}$ ), and (iii)  $x_t = f^t(x_0)$  (the  $t$ -th iterate of  $x_0 \in \Omega$  under  $f$ ). Suppose that the state space  $\Omega$  is discretized by the partition  $\mathcal{P} = \{P_1, P_2, \dots, P_{|\mathcal{P}|}\}$ , where  $P_k \in \mathcal{B}$  for  $k = 1, \dots, |\mathcal{P}|$ . If  $X_t^{\mathcal{P}} : \Omega \rightarrow \{1, \dots, |\mathcal{P}|\}$  are the mappings defined as

$$X_t^{\mathcal{P}}(x) = k \Leftrightarrow f^t(x) \in P_k, \quad (8)$$

then  $\mathbf{X}^{\mathcal{P}} : (X_t^{\mathcal{P}})_{t \geq 0}$  is a stationary random process with alphabet (or state space)  $\mathcal{A} = \{1, \dots, |\mathcal{P}|\}$ , called the *symbolic dynamics of  $f$  with respect to  $\mathcal{P}$* , whose probability distribution is given by<sup>2</sup>

$$\begin{aligned} \mathbb{P}(X_t^{\mathcal{P}} = k_0, X_{t+1}^{\mathcal{P}} = k_1, \dots, X_{t+n}^{\mathcal{P}} = k_n) \\ = \mu(P_{k_0} \cap f^{-1}(P_{k_1}) \cap \dots \cap f^{-n}(P_{k_n})). \end{aligned} \quad (9)$$

Therefore, the symbolic representation  $\alpha = (\alpha_t)_{t \geq 0}$  of  $x = (x_t)_{t \geq 0}$ , where  $\alpha_t = k \in \mathcal{A}$  if  $x_t = f^t(x_0) \in P_k$ , is, according to equation (8), a realization of the random process  $\mathbf{X}^{\mathcal{P}}$ . See the books by Kitchens<sup>36</sup> and Lind<sup>37</sup> for the general approach, and the book by Hao and Zhen<sup>38</sup> for applications of symbolic dynamics to Chaos Theory.

In particular, an ordinal representation of  $x$  is obtained by coarse-graining  $\Omega$  with the *ordinal partition*

$$\mathcal{P}_L = \{P_{\mathbf{r}} \neq \emptyset : \mathbf{r} \in \text{Sym}(L)\},$$

where

$$P_{\mathbf{r}} = \{x \in \Omega : \text{rank}(x, f(x), \dots, f^{L-1}(x)) = \mathbf{r}\}.$$

In nonlinear time series analysis, the probability of any outcome is estimated by their frequency (maximum likelihood estimator) in a statistically significant sample of symbolic series  $\mathbf{X}^{\mathcal{P}}(x_0) = (k_t)_{t \geq 0}$  (i.e., initial conditions  $x_0 \in \Omega$ ) or a long enough time series. The resulting measure  $\mu$ , equation (9), is called<sup>39</sup> the physical or natural measure of  $\Omega$ .

**Definition 3** A symbolic representation  $\alpha = (\alpha_t)_{t \geq 0}$  of a time series  $\mathbf{x} = (x_t)_{t \geq 0}$  is called an algebraic representation if the symbols  $\alpha_t$  are elements of a finite group  $(\mathcal{G}, \cdot)$ .

In addition to the group  $\text{Sym}(L)$  of the ordinal representation with embedding dimension  $L$ , examples of algebraic representations include  $\mathcal{G} = \{0, 1\}$  endowed with the XOR operation (addition modulo 2) and, more generally,  $\mathcal{G} = \{0, 1, \dots, n-1\}$  endowed with addition modulo  $n$ . These groups arise in digital communications and cryptography. Henceforth, all groups are finite.

**Remark 4** 1. Among the different algebraic symbols for the rank relationships (1) and (2) mentioned in Remark 1, only the 0-1 square matrices proposed by Bunk et al.<sup>22</sup> build a group (with respect to matrix multiplication). More generally, for a subset  $S$  of a group  $\mathcal{G}$  to be the alphabet of an algebraic representation,  $S$  must be a subgroup of  $\mathcal{G}$ .

2. A different situation occurs when the alphabet of a symbolic representation can be endowed with an algebraic structure. For example, the alphabet  $\mathcal{A} = \{1, \dots, |\mathcal{P}|\}$  of the symbolic dynamics with respect to a partition  $\mathcal{P}$ , equation (8), can be transformed into a group just by adding the letters modulo  $|\mathcal{P}|$ .

It is remarkable that, according to the following theorem of Group Theory, called the *Cayley theorem*<sup>12,16</sup>, permutations can be seen as universal symbols for algebraic representations.

**Theorem 5 (Cayley)** Every group  $(\mathcal{G}, \cdot)$  is isomorphic to a subgroup of  $(\text{Sym}(|\mathcal{G}|), *)$ , i.e., there is a mapping (called a group homomorphism)  $\Phi : \mathcal{G} \rightarrow \text{Sym}(|\mathcal{G}|)$  such that

**(P1):**  $\Phi$  sends the identity element  $e$  of  $\mathcal{G}$  to the identity permutation  $(1, 2, \dots, |\mathcal{G}|)$  of  $\text{Sym}(|\mathcal{G}|)$ ;

**(P2):**  $\Phi(a \cdot b) = \Phi(a) * \Phi(b)$  for all  $a, b \in \mathcal{G}$ . Hence,  $\Phi(a^{-1}) = (\Phi(a))^{-1}$ .

Therefore, if we restrict the range of the homomorphism  $\Phi$  to its image,  $\Phi(\mathcal{G})$ , we obtain a group isomorphism  $\mathcal{G} \rightarrow \Phi(\mathcal{G})$ , i.e., a bijective (one-to-one, invertible) homomorphism, called Cayley's isomorphism which, abusing notation, will also be denoted by  $\Phi$ . In this case,  $\mathcal{H} := \Phi(\mathcal{G})$  is a subgroup of  $\text{Sym}(|\mathcal{G}|)$  with cardinality  $|\mathcal{H}| = |\mathcal{G}|$ . Sometimes we also call the homomorphism  $\Phi : \mathcal{G} \rightarrow \text{Sym}(|\mathcal{G}|)$  an embedding.

In view of Cayley's theorem, any group  $\mathcal{G}$  can be represented by means of  $|\mathcal{G}|$  permutations on the set  $\{1, 2, \dots, |\mathcal{G}|\}$ . From a practical point of view, finding the minimal-order symmetric group into which a given group  $\mathcal{G}$  embeds in  $\text{Sym}(\mathcal{G})$  is rather difficult<sup>40,41</sup>. On the other hand, Cayley's theorem is practical when it comes to endow groups of low and moderate cardinality with a metric, as we will discuss in Section V F.

Cayley's isomorphism can be implemented in several ways. In Section IV we are going to learn some of them.

## IV. TRANSCRIPTS

Ordinal representations are very popular in time series analysis<sup>42,43</sup>. However, very few applications have harnessed the algebraic structure of the symmetric group so far. In fact, the only applications we are aware of build on the concept of transcript, introduced by Monetti et al.<sup>14</sup>. In this section, we consider this concept in the more general framework of algebraic representations and discuss its main properties, before revisiting some applications in Section V.

**Definition 6** Given a finite group  $(\mathcal{G}, \cdot)$ , the transcription mapping  $T : \mathcal{G} \times \mathcal{G} \rightarrow \mathcal{G}$  is defined as

$$T(a, b) = b \cdot a^{-1}. \quad (10)$$

The group element  $T(a, b)$  is called the transcript from the source  $a$  to the target  $b$ .

The basic properties of the transcription mapping are the following.

**(T1):**  $T(b, a) = T(a, b)^{-1}$ .

**(T2):**  $T(b, c) \cdot T(a, b) = T(a, c)$ .

**(T3):**  $T$  is a  $|\mathcal{G}|$ -to-1 mapping. In fact, for  $\forall c \in \mathcal{G}$ ,

$$T^{-1}(c) = \{(a, c \cdot a), \forall a \in \mathcal{G}\} = \{(c^{-1} \cdot b, b), \forall b \in \mathcal{G}\}.$$

Trivially, the sets  $\{T^{-1}(c) : c \in \mathcal{G}\}$  build a partition of  $\mathcal{G} \times \mathcal{G}$ .

**(T4): Equivalence property.** Given a triple  $(a, b, T(a, b))$ , any pair of elements (i.e.,  $(a, b)$ ,  $(a, T(a, b))$  or  $(b, T(a, b))$ ) univocally determines the remaining element. This property is instrumental in many proofs involving transcripts.

**Example 7** For  $\mathcal{G} = \text{Sym}(3)$ , we obtain the following transcripts  $T(\mathbf{r}, \mathbf{s}) = \mathbf{s} * \mathbf{r}^{-1}$ ,

$\mathbf{s} * \mathbf{r}^{-1}$	123	132	213	231	312	321
123	123	132	213	231	312	321
132	132	123	312	321	213	231
213	213	231	123	132	321	312
231	312	321	132	123	231	213
312	231	213	321	312	123	132
321	321	312	231	213	132	123

where the source permutation  $\mathbf{r}$  labels the rows and the target permutation  $\mathbf{s}$  labels the columns.

If  $(\mathcal{G}, \cdot)$  is non-abelian, a *conjugate transcription mapping*  $\tilde{T} : \mathcal{G} \times \mathcal{G} \rightarrow \mathcal{G}$  can be defined as

$$\tilde{T}(a, b) = a^{-1} \cdot b. \quad (11)$$

Note that

$$\tilde{T}(a, b) = T(b^{-1}, a^{-1}). \quad (12)$$

The transformation  $\tilde{T}_a := \tilde{T}(a, \cdot) : \mathcal{G} \rightarrow \mathcal{G}$ , i.e.,

$$\tilde{T}_a(b) := \tilde{T}(a, b) = a^{-1} \cdot b \quad (13)$$

is called a *left translation* by  $a$ .

The following result shows how to implement Cayley's isomorphism via conjugate transcripts.

**Theorem 8** For each  $a \in \mathcal{G}$ , the mapping  $\Phi : a \mapsto \tilde{T}_a = \tilde{T}(a, \cdot)$  is an isomorphism from  $(\mathcal{G}, \cdot)$  onto a subgroup of  $(\text{Sym}(\mathcal{G}), *)$ .

**Proof.** First of all, we show that  $\tilde{T}_a \in \text{Sym}(\mathcal{G})$ , i.e., it is a bijection from  $\mathcal{G}$  to  $\mathcal{G}$ , for all  $a \in \mathcal{G}$ . This is true because every  $b \in \mathcal{G}$  has an inverse (or anti-image) under  $\tilde{T}_a$ , namely,  $(\tilde{T}_a(b))^{-1} = \tilde{T}_{a^{-1}}(b)$ . Indeed,

$$(\tilde{T}_a * \tilde{T}_{a^{-1}})(b) = \tilde{T}_{a^{-1}}(\tilde{T}_a(b)) = a \cdot (a^{-1} \cdot b) = (a \cdot a^{-1}) \cdot b = b$$

for all  $b \in \mathcal{G}$ . Analogously,  $\tilde{T}_{a^{-1}} * \tilde{T}_a = \text{id}$ .

To show that  $\Phi : a \mapsto \tilde{T}_a$  is a group homomorphism from  $\mathcal{G}$  into  $\text{Sym}(\mathcal{G})$ , we have to prove that Properties (P1) and (P2) in Theorem 5 hold true.

(P1) Let  $e$  be the identity element of  $\mathcal{G}$ . Then,  $\tilde{T}_e(a) = e^{-1} \cdot a = a$  for all  $a \in \mathcal{G}$ , which shows that  $\tilde{T}_e : \mathcal{G} \rightarrow \mathcal{G}$  is the identity mapping.

(P2) Furthermore,

$$\begin{aligned} \tilde{T}_{a \cdot b}(c) &= (a \cdot b)^{-1} \cdot c = (b^{-1} \cdot a^{-1}) \cdot c = b^{-1} \cdot (a^{-1} \cdot c) \\ &= \tilde{T}_b(\tilde{T}_a(c)) = (\tilde{T}_a * \tilde{T}_b)(c) \end{aligned}$$

for all  $a, b, c \in \mathcal{G}$ .

Hence,  $\mathcal{G}$  is isomorphic to its image  $\Phi(\mathcal{G})$  under  $\Phi$ . ■

The implementation  $\Phi : a \mapsto \tilde{T}_a$  of Cayley's isomorphism, Theorem 8, can be visualized as follows. Let  $\{a_1, a_2, \dots, a_n\}$  be any ordering of the elements of  $\mathcal{G}$ , so that the conjugate transcription mapping  $\tilde{T} : \mathcal{G} \times \mathcal{G} \rightarrow \mathcal{G}$  can be represented by the  $n \times n$  matrix  $(\tilde{T}(a_i, a_j))_{1 \leq i, j \leq n}$ , shortened as  $(\tilde{T}(i, j))_{1 \leq i, j \leq n} = (\tilde{T}_i(j))_{1 \leq i, j \leq n}$  in the following table:

$$\begin{array}{c|cccc} & 1 & \cdots & j & \cdots & n \\ \hline 1 & \tilde{T}_1(1) & \cdots & \tilde{T}_1(j) & \cdots & \tilde{T}_1(n) \\ \vdots & \vdots & \vdots & \vdots & \vdots & \vdots \\ i & \tilde{T}_i(1) & \cdots & \tilde{T}_i(j) & \cdots & \tilde{T}_i(n) \\ \vdots & \vdots & \vdots & \vdots & \vdots & \vdots \\ n & \tilde{T}_n(1) & \cdots & \tilde{T}_n(j) & \cdots & \tilde{T}_n(n) \end{array} \quad (14)$$

Therefore, the  $i$ th row of the conjugate transcription matrix (14) is precisely the one-line form of the permutation  $\tilde{T}_i := \tilde{T}(i, \cdot)$ ,  $1 \leq i \leq n$ :

$$\Phi(a_i) = \tilde{T}_{a_i} \equiv \tilde{T}_i = \left( \begin{array}{cccc} 1 & \cdots & j & \cdots & n \\ \tilde{T}_i(1) & \cdots & \tilde{T}_i(j) & \cdots & \tilde{T}_i(n) \end{array} \right). \quad (15)$$

**Example 9** Let us particularize the procedure (14)-(15) to the Klein four-group  $(\mathcal{K}, \cdot)$ , defined by the multiplication table

$$\begin{array}{c|cccc} \cdot & e & a & b & c \\ \hline e & e & a & b & c \\ a & a & e & c & b \\ b & b & c & e & a \\ c & c & b & a & e \end{array} \quad (16)$$

Note that  $\mathcal{K}$  is abelian (as any group whose cardinality is the square of a prime number) since the multiplication table in equation (16) is symmetric and every element other than the identity  $e$  has order 2, i.e., every element is its own inverse. Therefore,  $\tilde{T}_r(s) = r^{-1} \cdot s = r \cdot s$  for all  $r, s \in \mathcal{K}$ , so that the table for the left translations  $\tilde{T}_r \in \text{Sym}(\mathcal{K}) = \text{Sym}(4)$  is obtained by just copying the multiplication table (16):

$$\begin{array}{c|cccc} & e & a & b & c \\ \hline \tilde{T}_e & e & a & b & c \\ \tilde{T}_a & a & e & c & b \\ \tilde{T}_b & b & c & e & a \\ \tilde{T}_c & c & b & a & e \end{array} \quad (17)$$

Thus, the isomorphic copy  $\tilde{T}_b$  of  $b \in \mathcal{K}$  is the permutation given by the third row of the table in equation (16):

$$\tilde{T}_b = \begin{pmatrix} e & a & b & c \\ b & c & e & a \end{pmatrix} = bcea. \quad (18)$$

If the elements of  $\mathcal{K}$  are encoded as, say,

$$e = 1, a = 2, b = 3, c = 4, \quad (19)$$

then

$$\tilde{T}_1 = 1234, \tilde{T}_2 = 2143, \tilde{T}_3 = 3412, \tilde{T}_4 = 4321. \quad (20)$$

The concept of transcription translates to time series in a straightforward way. Let  $x = (x_t)_{t \geq 0}$  and  $y = (y_t)_{t \geq 0}$  be two time series and let  $\alpha = (\alpha_t)_{t \geq 0}$  and  $\beta = (\beta_t)_{t \geq 0}$  be algebraic representations of  $x$  and  $y$  over the same group  $\mathcal{G}$ . Remember that  $\alpha$  and  $\beta$  are  $\mathcal{G}$ -valued random trajectories (Section III).

**Definition 10** Let  $T : \mathcal{G} \times \mathcal{G} \rightarrow \mathcal{G}$  be the transcription mapping defined in Definition 6. The transcription with source  $\alpha$ , target  $\beta$ , and coupling delay  $\Lambda \in \mathbb{Z}$  is the  $\mathcal{G}$ -valued time series

$$T_{\alpha, \beta_\Lambda} = (T(\alpha_t, \beta_{t+\Lambda}))_{t \geq t_0} = (\beta_{t+\Lambda} * \alpha_t^{-1})_{t \geq t_0} \quad (21)$$

where  $t_0 = \max\{0, -\Lambda\}$ .

Without loss of generality, we apply the coupling delay to the target (see property (T1) above). If the source and target are known from the context, we will shorten  $T_{\alpha, \beta_\Lambda} = (\beta_{t+\Lambda} * \alpha_t^{-1})_{t \geq t_0}$  as

$$T_{\alpha, \beta_\Lambda} = (\tau_t(\Lambda))_{t \geq t_0}, \quad (22)$$

with

$$\tau_t(\Lambda) := \beta_{t+\Lambda} * \alpha_t^{-1} \in \mathcal{G}. \quad (23)$$

If  $\Lambda = 0$ , then we set  $\tau_t(0) = \tau_t = \beta_t * \alpha_t^{-1}$ .

The fact that  $t_0 = |\Lambda| > 0$  for  $\Lambda < 0$  is irrelevant in practice. Alternatively, in that case one could set  $\beta_{-|\Lambda|} = \beta_{-|\Lambda|+1} = \dots = \beta_{-1} := e$  and start at  $t = 0$  in Equation (21), as we will do from now on for notational simplicity. If  $y = x$  and  $\Lambda \neq 0$ , then we call  $\tau_t(\Lambda) = \alpha_{t+\Lambda} * \alpha_t^{-1}$ ,  $t \geq 0$ , *self-transcripts*; otherwise, if  $y \neq x$  and  $\Lambda \in \mathbb{Z}$ , we speak of *cross-transcripts* or simply transcripts. As its name indicates, the coupling delay  $\Lambda$  allows us to study the dependencies between different variables of a time series (self-transcripts) or two time series (cross-transcripts).

Definition 10 can be generalized to more than two algebraic representations over of the same group. Thus, if  $\alpha^m = (\alpha_t^m)_{t \geq 0}$ ,  $m = 1, 2, \dots, M \geq 2$ , are  $\mathcal{G}$ -valued representations, then we can define a (self- or cross-) transcription for any of the  $M^2$  possible pairings  $\alpha^j, \alpha^k$  of the algebraic representations  $\alpha^1, \dots, \alpha^M$ :

$$T_{\alpha^j, \alpha^k_{\Lambda(j,k)}} = (T(\alpha_t^j, \alpha_{t+\Lambda(j,k)}^k))_{t \geq 0}, \quad (24)$$

where we allow for coupling delays that depend on the source and the target. Abusing notation, we will use the notations  $\alpha^j, \alpha^k_{\Lambda(j,k)}, T_{\alpha^j, \alpha^k_{\Lambda(j,k)}}$  and the like for both time series and  $\mathcal{G}$ -valued random processes that generate them.

## V. TRANSCRIPT-BASED TOOLS AND APPLICATIONS

In this section we review several transcript-based tools in use in time series analysis. The traditional tools include the entropic (Sections V A-V C) and algebraic (V D) ones. The most recent tools are the Cayley and Kendall distances between permutations (V E) and their extensions to general groups (Section V F), which also fall into the category of algebraic tools. The noise robustness of transcript-based tools has been studied by Adams and Lehnertz<sup>44</sup>. For the information-theoretic concepts below, see the book by Cover and Thomas<sup>45</sup>.

### A. Entropy

One of the main tools in nonlinear time series analysis is entropy. Let  $\alpha = (\alpha_t)_{t \geq 0}$ ,  $\beta = (\beta_t)_{t \geq 0}$  be two stationary  $\mathcal{G}$ -valued random processes, and  $T_{\alpha, \beta_\Lambda} = (T_{\alpha, \beta_{t+\Lambda}})_{t \geq 0}$  the random process defined in equations (21)-(23)). The *transcript entropy* of the source process  $\alpha$  and target process  $\beta$  with coupling delay  $\Lambda \in \mathbb{Z}$  is the Shannon entropy of the random variable  $T_{\alpha, \beta_{t+\Lambda}} = \beta_{t+\Lambda} * \alpha_t^{-1}$  with probability distribution  $P_\tau(\Lambda) = \{p(\tau_t(\Lambda)) : \tau_t(\Lambda) \in \mathcal{G}\}$ , i.e.,

$$H(T_{\alpha, \beta_{t+\Lambda}}) = H(P_\tau(\Lambda)) = - \sum_{\tau_t(\Lambda) \in \mathcal{G}} p(\tau_t(\Lambda)) \log p(\tau_t(\Lambda)), \quad (25)$$

where  $t$  is fixed but otherwise arbitrary due to stationarity,

$$p(\tau_t(\Lambda)) = \sum_{\beta_{t+\Lambda} * \alpha_t^{-1} = \tau_t(\Lambda)} p(\alpha_t, \beta_{t+\Lambda}) = \sum_{\alpha_t \in \mathcal{G}} p(\alpha_t, \tau_t(\Lambda) * \alpha_t), \quad (26)$$

$p(\alpha_t, \beta_{t+\Lambda})$  being the joint probability of the symbols  $\alpha_t$  and  $\beta_{t+\Lambda}$ . The usual logarithm bases are  $e$  and 2.

In the particular case  $\beta = \alpha$  and  $\Lambda \neq 0$ , we speak of the self-transcript entropy  $H(T_{\alpha, \alpha_{t+\Lambda}})$  of the random process  $\alpha$  with coupling delay  $\Lambda$ ; otherwise we speak of cross-transcript entropy or simply transcript entropy. By property (T1) of Section IV,  $H(T_{\alpha, \beta_{t+\Lambda}}) = H(T_{\beta_{t+\Lambda}, \alpha_t})$ . On the other hand,  $H(T_{\alpha, \beta_{t+\Lambda}}) \neq H(T_{\alpha_{t+\Lambda}, \beta_t})$  in general, unless  $\Lambda = 0$ .

Since  $H(T_{\alpha, \beta_{t+\Lambda}})$  ranges between 0 and  $\log |\mathcal{G}|$ , the normalized entropy

$$h(T_{\alpha, \beta_{t+\Lambda}}) := \frac{H(T_{\alpha, \beta_{t+\Lambda}})}{\log |\mathcal{G}|} = \frac{H(P_\tau(\Lambda))}{\log |\mathcal{G}|} =: h(P_\tau(\Lambda)) \quad (27)$$

is preferred in applications. If  $\Lambda = 0$ , we write  $P_\tau(0) = P_\tau = \{p(\tau_t) : \tau_t \in \mathcal{G}\}$ .

More generally, the Shannon entropy of a probability distribution of ordinal patterns is called permutation entropy<sup>10,46</sup>. Of course, the Shannon entropy can be replaced by any other entropy in the equation (25), in particular by the Rényi or Tsallis entropies<sup>47,48</sup>, which are one-parameter families of generalized entropies that include the Shannon entropy.

In the case of drive-response systems, the driver may have forbidden symbols, as actually happens in the ordinal representations. However, this does not mean that there will also be forbidden transcripts because, as shown in Section III, there are  $|\mathcal{G}|$  pairs  $(\alpha_t, \beta_{t+\Lambda})$  such that  $\beta_{t+\Lambda} * \alpha_t^{-1} = \tau_t(\Lambda)$ . So, we expect that, in general,  $p(\tau_t(\Lambda)) > 0$  for all  $\tau_t(\Lambda) \in \mathcal{G}$ . There are exceptions, though: full and generalized synchronization. We come back to this point in Section VI C.

Transcript entropy has been used to study the brain activity of a subject suffering from frontal lobe epilepsy<sup>15</sup>.

Differentiation of patients with obstructive sleep apnea from healthy controls has been achieved based on the heart rate–blood pressure coupling quantified by entropic indices, including self- and cross-transcript entropies<sup>49</sup>. Remarkably, all 10 best triplets of classifiers include the self-transcript entropy of the heart-rate time series with different patterns lengths and coupling delays.

Entropy is instrumental for calculating divergences, statistical complexity, coupling complexity coefficients, and mutual information in the forthcoming Sections V B-V C. For the estimation of entropy in time series analysis, see Paninski<sup>50</sup>. For practical considerations of permutation entropy, see Riedl et al.<sup>51</sup>. The statistical properties of permutation entropy are studied in Chagas et al.<sup>52</sup>.

### B. Divergence and statistical complexity

Again, let  $P_\tau = \{p(\tau_t) : \tau_t \in \mathcal{G}\}$  be a (theoretical or empirical) probability distribution of transcripts obtained from two stationary  $\mathcal{G}$ -valued random processes  $\alpha = (\alpha_t)_{t \geq 0}$ ,  $\beta = (\beta_t)_{t \geq 0}$  as in equation (26), and  $Q^{\text{ref}} = \{q(\tau_t) : \tau_t \in \mathcal{G}\}$  be a “reference” probability distribution. In case of a coupling delay  $\Lambda \neq 0$ , replace  $\tau_t$  by  $\tau_t(\Lambda)$ .

The *Kullback-Leibler (KL) divergence* (or relative entropy) of  $P_\tau$  and  $Q^{\text{ref}}$ , a type of statistical distance or a measure of

similarity between probability distributions, is defined as

$$D_{KL}(P_\tau \parallel Q^{\text{ref}}) = \sum_{\tau_i \in \mathcal{G}} p(\tau_i) \log \frac{p(\tau_i)}{q(\tau_i)}. \quad (28)$$

Note that  $D_{KL}(P_\tau \parallel Q^{\text{ref}})$  is in general not symmetric with respect to the exchange of  $P_\tau$  and  $Q^{\text{ref}}$ . Therefore, a symmetrized form  $D_{KL}^{\text{sym}}(P_\tau \parallel Q^{\text{ref}})$ , such as the arithmetic or harmonic mean of  $D_{KL}(P_\tau \parallel Q^{\text{ref}})$  and  $D_{KL}(Q^{\text{ref}} \parallel P_\tau)$ , is preferred in practice.

But perhaps the most popular symmetric divergence currently is the *Jensen-Shannon (JS) divergence*, which, particularized to the probabilities  $P_\tau$  and  $Q^{\text{ref}}$ , is defined as

$$D_{JS}(P_\tau \parallel Q^{\text{ref}}) = H\left(\frac{P_\tau + Q^{\text{ref}}}{2}\right) - \frac{1}{2}\left(H(P_\tau) + H(Q^{\text{ref}})\right), \quad (29)$$

where  $H(\cdot)$  is the Shannon entropy. Among its properties we highlight: (i)  $0 \leq D_{JS}(P \parallel Q) \leq \log 2$  for any two probability distributions  $P$  and  $Q$  on the same finite state space (so that the JS divergence ranges in the interval  $[0, 1]$  if base 2 logarithms are used<sup>53</sup>), (ii) the maximum value is achieved when  $P$  and  $Q$  have disjoint supports (meaning there is no event where both  $P$  and  $Q$  assign a non-zero probability), and (iii)  $(D_{JS}(P \parallel Q))^{1/2}$  is formally a distance for probability distributions, called the Jensen-Shannon distance<sup>54</sup>.

Several choices are common for  $Q^{\text{ref}}$ . The simplest one is the uniform distribution  $U$  on  $\mathcal{G}$ . Another choice is  $P_\tau^{\text{ind}} = \{p_{\text{ind}}(\tau_i) : \tau_i \in \mathcal{G}\}$ , where<sup>14</sup>

$$p_{\text{ind}}(\tau_i) = \sum_{\beta_t * \alpha_t^{-1} = \tau_i} p(\alpha_t)p(\beta_t) \quad (30)$$

and  $t$  is fixed but otherwise arbitrary due to the assumed stationarity of the time series. In other words, if  $P_\alpha = \{p(\alpha_t) : \alpha_t \in \mathcal{G}\}$  and  $P_\beta = \{p(\beta_t) : \beta_t \in \mathcal{G}\}$ , then  $P_\tau^{\text{ind}}$  is the probability distribution obtained from the product distribution  $P_\alpha \times P_\beta$  by adding the entries  $p(\alpha_t)p(\beta_t)$  such that  $\beta_t * \alpha_t^{-1} = \tau_i$  for each  $\tau_i \in \mathcal{G}$ . Therefore,  $D_{JS}(P_\tau \parallel P_\tau^{\text{ind}})$  and  $D_{JS}(P_\tau \parallel P_\tau^{\text{ind}})^{1/2}$  can be considered nonlinear measures of statistical dependence between the processes  $\alpha$  and  $\beta$ .

The product of the JS divergence  $D_{JS}(P \parallel U)$  (where  $P$  stands for any probability distribution) times the Shannon entropy  $H(P)$  was introduced by Rosso et al.<sup>55</sup> and called the *statistical complexity* of the probability distribution  $P$ ,

$$\text{SC}(P) = D_{JS}(P \parallel U)H(P). \quad (31)$$

Usually, definition (31) is provided with an additional normalization factor. Of course, if base 2 logarithms are used (so that  $0 \leq D_{JS}(P \parallel U) \leq 1$ ) and  $H(P)$  is replaced with the normalized entropy  $h(P) = H(P)/\log_2 |\mathcal{G}|$  (equation (27)), then  $0 \leq \text{SC}(P) \leq 1$  automatically. By definition,  $\text{SC}(P) = 0$  when  $P$  is uniform ( $P = U$ ) or when  $P$  is deterministic, reaching its maximum between those extreme situations.

Analogously, we call

$$\text{SC}(P_\tau, Q^{\text{ref}}) = D^{\text{sym}}(P_\tau \parallel Q^{\text{ref}})H(P_\tau) \quad (32)$$

(possibly with a normalization factor) the *transcript statistical complexity* of the transcript probability distribution  $P_\tau$  with respect to  $Q^{\text{ref}}$ , where  $D^{\text{sym}}(P_\tau \parallel Q^{\text{ref}})$  is a divergence symmetric in  $P_\tau$  and  $Q^{\text{ref}}$ .

Usually,  $D^{\text{sym}}(P_\tau \parallel Q^{\text{ref}})$  is the JS divergence but other choices have been used in the literature, too. Thus, the harmonic mean

$$D_{KL}^{\text{sym}}(P_\tau \parallel P_\tau^{\text{ind}}) = \frac{D_{KL}(P_\tau \parallel P_\tau^{\text{ind}})D_{KL}(P_\tau^{\text{ind}} \parallel P_\tau)}{D_{KL}(P_\tau \parallel P_\tau^{\text{ind}}) + D_{KL}(P_\tau^{\text{ind}} \parallel P_\tau)}$$

has been used<sup>14</sup> to characterize the synchronization regimes of a bidirectionally coupled Rössler-Rössler system.

Likewise,  $\text{SC}_{KL}(P_\tau, P_\tau^{\text{ind}}) = D_{KL}^{\text{sym}}(P_\tau \parallel P_\tau^{\text{ind}})H(P_\tau)$  has been used<sup>15</sup> to measure the complexity of two bidirectionally coupled Rössler oscillators and two delay-coupled logistic maps.

### C. Mutual information and coupling complexity coefficients

Given  $M \geq 2$  stationary  $\mathcal{G}$ -valued random processes  $\alpha^m = (\alpha_t^m)_{t \geq 0}$ ,  $1 \leq m \leq M$ , their *coupling complexity coefficient* (CCC) is defined as<sup>56,57</sup>

$$C(\alpha^1, \dots, \alpha^M) = \min_{1 \leq m \leq M} I(\alpha_t^m; T_{\alpha_t^1, \alpha_t^2, \dots, \alpha_t^{M-1}, \alpha_t^M}), \quad (33)$$

where  $T_{\alpha_t^m, \alpha_t^{m+1}}$  is the random variable  $\tau_t^{m, m+1} = \alpha_t^{m+1} * (\alpha_t^m)^{-1}$ ,  $1 \leq m \leq M-1$ , and  $I(\cdot; \cdot)$  is the mutual information of its (scalar or vectorial) arguments. By definition,  $C(\alpha^1, \dots, \alpha^M) \geq 0$ . There are other equivalent definitions<sup>56,57</sup>. For example, in the two-dimensional case,

$$\begin{aligned} C(\alpha^1, \alpha^2) &= \min\{I(\alpha_t^1; T_{\alpha_t^1, \alpha_t^2}), I(\alpha_t^2; T_{\alpha_t^1, \alpha_t^2})\} \\ &= \min\{H(\alpha_t^1), H(\alpha_t^2)\} - H(\alpha_t^1, \alpha_t^2) + H(T_{\alpha_t^1, \alpha_t^2}) \\ &= H(T_{\alpha_t^1, \alpha_t^2}) - \max\{H(\alpha_t^1 | \alpha_t^2), H(\alpha_t^2 | \alpha_t^1)\}. \end{aligned}$$

The name CCC is justified by the following two properties<sup>56</sup>:

- (i): If  $\alpha^1 = \alpha^2 = \dots = \alpha^M$ , then  $C(\alpha^1, \dots, \alpha^M) = 0$ .
- (ii): If  $\alpha^1, \alpha^2, \dots, \alpha^M$  are independent and uniformly distributed, then  $C(\alpha^1, \dots, \alpha^M) = 0$ .

So,  $C(\alpha^1, \dots, \alpha^M) > 0$  in “nontrivial” situations. Among other properties of  $C(\alpha^1, \dots, \alpha^M)$ , we mention two more here:

- (iii): *Invariance*<sup>56</sup>.  $C(\alpha^1, \dots, \alpha^M)$  is invariant under permutations of  $\alpha^1, \dots, \alpha^M$ .

- (iv): *Monotonicity*<sup>56</sup>.  $C(\alpha^1, \dots, \alpha^k, \dots, \alpha^M) < C(\alpha^1, \dots, \alpha^{k-1}, \alpha^{k+1}, \dots, \alpha^M)$  is only possible when  $H(\alpha^k)$  is the unique minimum of all the entropies  $H(\alpha^m)$ ,  $1 \leq m \leq M$ ; otherwise,  $C(\alpha^1, \dots, \alpha^k, \dots, \alpha^M) \geq C(\alpha^1, \dots, \alpha^{k-1}, \alpha^{k+1}, \dots, \alpha^M)$ .

Furthermore, numerical simulations<sup>57</sup> with ordinal representations of time series indicate that  $C(\alpha^1, \dots, \alpha^M)$  is monotonically decreasing with respect to the delay time  $T$  (see Equation (2)), i.e.,  $C(\alpha^1, \dots, \alpha^M) \searrow 0$  when  $T \rightarrow \infty$ . This property has been applied in the so-called *dimensional reduction of the conditional mutual information*. In its lowest dimensional version, this result states that

$$I(\beta_{t+\Lambda}; \alpha_t | \beta_t) = I(T_{\beta_{t+\Lambda}, \beta_t}; T_{\alpha_t, \beta_t}), \quad (34)$$

provided that  $H(\beta_t) \leq H(\alpha_t)$ , and  $C(\beta_\Lambda, \beta, \alpha) = 0$ , which, as said above, can be approximately achieved by fine-tuning the delay time. Here, (i)  $\Lambda \geq 1$ , (ii) the conditional mutual information on the lhs of (34) is, by definition, the *symbolic transfer entropy*<sup>58</sup> from the process  $\alpha$  to the process  $\beta$  with coupling delay  $\Lambda$ ,

$$I(\beta_{t+\Lambda}; \alpha_t | \beta_t) =: \text{TE}_{\alpha \rightarrow \beta}(\Lambda), \quad (35)$$

and (iii) the mutual information between transcripts on the rhs of (34) is called the *transcript mutual information* with coupling delay  $\Lambda$ ,

$$I(T_{\beta_{t+\Lambda}, \beta_t}; T_{\alpha_t, \beta_t}) =: \text{TMI}_{\alpha \rightarrow \beta}(\Lambda). \quad (36)$$

The transfer entropy  $\text{TE}_{\alpha \rightarrow \beta}(\Lambda)$  is a measure of the information transfer from  $\alpha$  to  $\beta$  (usually  $\Lambda = 1$ ). It is easy to check that  $\text{TE}_{\alpha \rightarrow \beta}(\Lambda) = \text{TMI}_{\alpha \rightarrow \beta}(\Lambda) = 0$  if  $\alpha = \beta$ , e.g., when the underlying dynamical systems are fully synchronized. See Amigó et al.<sup>9</sup> for the higher dimensional version of equation (34).

Among the applications of the CCC and the dimensional reduction (34) of the symbolic transfer entropy via transcripts, let us mention a few. So, the directionality indicator

$$\Delta T I_{\alpha \rightarrow \beta} = \text{TMI}_{\alpha \rightarrow \beta}(\Lambda) - \text{TMI}_{\beta \rightarrow \alpha}(\Lambda) \quad (37)$$

has been used as an information directionality index between (i) the lateral geniculate nucleus of the thalamus and the visual cortex infragranular layers<sup>59</sup> and (ii) heart rate and blood pressure with medical air breathing or oxygen breathing<sup>9</sup>, as well as to study the information directionality between two bidirectionally delay-coupled logistic maps<sup>9</sup>.

Transcript mutual information has been used as a causality index with ice core atmospheric data, as well as brain data during a visually cued, two-choice arm reaching task<sup>60</sup>.

The coupling complexity coefficient  $C(\alpha, \beta)$  and the directionality indicator (37) have been used to study the dynamics of two, unidirectionally coupled Hénon maps and Rössler oscillators, as well as to characterize brain-wide interactions during wakefulness and sleep<sup>61</sup>.

#### D. Order classes

The order (or period) of a symbol  $a \in \mathcal{G}$ ,  $\text{ord}(a)$ , is the minimum positive integer  $m$  such that  $a^m = e$ , the identity of  $\mathcal{G}$ . Three basic properties of  $\text{ord}(a)$  are the following<sup>12</sup>:

**(O1):** The only element of  $\mathcal{G}$  with order 1 is the identity  $e$ .

**(O2):**  $\text{ord}(a)$  is a divisor of  $|\mathcal{G}|$  for all  $a \in \mathcal{G}$ . In symbols:  $\text{ord}(a) \mid |\mathcal{G}|$ .

**(O3):**  $\text{ord}(a) = \text{ord}(a^{-1})$  for all  $a \in \mathcal{G}$ .

We define the *order class*  $\mathcal{C}_m$  as the subset of  $\mathcal{G}$  that comprises all elements of order  $m$ ,

$$\mathcal{C}_m = \{a \in \mathcal{G} : \text{ord}(a) = m\}, \quad (38)$$

where  $m \geq 1$  divides  $|\mathcal{G}|$ . In particular,  $\mathcal{C}_1 = \{e\}$  and  $\mathcal{C}_2 = \{a \in \mathcal{G} : a = a^{-1}\}$ .

The sets  $\mathcal{C}_m$  build a partition of  $\mathcal{G}$ . If  $|\mathcal{G}|$  is a prime number  $p$ , then  $\mathcal{G} = \mathcal{C}_1 \cup \mathcal{C}_p$ , i.e.,  $\mathcal{C}_p = \mathcal{G} \setminus \{e\}$ , which means that the group is cyclic (generated by the powers of any element  $a \neq e$ , with  $a^0 := e$ ).

By properties (T1) in Section IV and (O3) above, the order of the transcripts  $T_{a,b}$  are invariant under the exchange of the source  $a$  and the target  $b$ , i.e.,  $\text{ord}(T_{a,b}) = \text{ord}(T_{b,a})$ . The order of the transcript  $T_{a,b}$  was proposed as a measure of dissimilarity between  $a$  and  $b$  by Monetti et al.<sup>14</sup>. In Remark 16, equation (70), we will see that  $\text{ord}(T_{a,b}) - 1$  is actually a distance when  $\mathcal{G} = \text{Sym}(3)$ .

In time series analysis of coupled  $\mathcal{G}$ -valued time series  $\alpha = (\alpha_t)_{t \geq 0}$  and  $\beta = (\beta_t)_{t \geq 0}$ , we are interested in the order classes of their transcription  $\mathbf{T}_{\alpha, \beta_\Lambda} = (\tau_t(\Lambda))_{t \geq 0} = (\beta_{t+\Lambda} * \alpha_t^{-1})_{t \geq 0}$ . Again, the order classes of the transcripts are invariant under the exchange of the source  $\alpha$  and the target  $\beta$ .

More interesting from a physical point of view, it was observed by Monetti et al.<sup>14</sup> that the dynamics of coupled nonlinear systems can lead to the extinction of transcript order classes, a phenomenon called saturation. As a trivial example, if  $\alpha$  and  $\beta$  are algebraic representations of a fully synchronized drive-response system, then  $\mathcal{C}_m = \emptyset$  for all  $m \neq 1$  because then  $\beta = \alpha$  and, hence,  $\tau_t = \alpha_t * \alpha_t^{-1} = e$  for all  $t \geq 0$ . Non-trivial examples can arise in case of generalized synchronization, as we will see in Section VIC.

Although any transcript-based entropic measure is in principle sensitive to saturation in coupled dynamics, there are tools tailored to this end. For example, the transcript probabilities  $p(\tau)$  and  $p^{\text{ind}}(\tau)$  can be lumped by order class. In such a case:

(a)  $P_\tau = \{p(\tau_t) : \tau_t \in \mathcal{G}\}$  changes to  $P_\tau^\mathcal{C} = \{p_{\mathcal{C}_m} : m \mid |\mathcal{G}|\}$ , where

$$p_{\mathcal{C}_m} = \sum_{\tau \in \mathcal{C}_m} p(\tau). \quad (39)$$

(b)  $P_\tau^{\text{ind}}$  changes to  $P_\tau^{\mathcal{C}, \text{ind}} = \{p_{\mathcal{C}_m, \text{ind}} : m \mid |\mathcal{G}|\}$ , where

$$p_{\mathcal{C}_m, \text{ind}} = \sum_{\tau \in \mathcal{C}_m} p^{\text{ind}}(\tau) \quad (40)$$

and  $p^{\text{ind}}(\tau)$  is given in equation (30).

The divergences  $D_{KL}^{\text{sym}}(P_\tau^\mathcal{C} \parallel P_\tau^{\mathcal{C}, \text{ind}})$  and the probabilities  $p_{\mathcal{C}_m}$  (with ordinal patterns of lengths 6 and 7) have been used<sup>14</sup> to characterize the synchronization regimes of a bidirectionally coupled Rössler-Rössler system. A similar study has also been performed<sup>22</sup> with the frequencies of order classes and patterns of length 6.

Likewise, the divergence  $D_{JS}(P_{\tau}^{\mathcal{C}} \| P_{\tau}^{\mathcal{C}, \text{ind}})$  and the probabilities  $p_{\mathcal{C}_m}$  (with ordinal patterns of length 4) have been used<sup>61</sup> to study the dynamics of two, unidirectionally coupled Hénon maps and Rössler oscillators, as well as to characterize brain-wide interactions during wakefulness and sleep.

### E. Distances in the symmetric groups

An edit distance between two strings of symbols is defined as the minimum number of allowed edit operations (insertions, deletions, substitutions, transpositions) to transform one string into the other. Since permutations, written in one-line form, are symbolic strings without repeated symbols, any suitable edit distance can be used to measure the distance between them, as proposed by Sörensen<sup>62</sup>.

The perhaps most important edit distances for the symmetric groups  $\text{Sym}(L)$  are the Cayley distance<sup>63</sup> and the Kendall (tau-) distance<sup>64</sup>, where the allowed operations are transpositions and adjacent transpositions of symbols, respectively. Specifically, transpositions are cycles of length 2, i.e., a transposition  $(ij)$  is a permutation  $\mathbf{t}_{ij} \in \text{Sym}(L)$  such that  $\mathbf{t}_{ij}(i) = j$ ,  $\mathbf{t}_{ij}(j) = i$ , and  $\mathbf{t}_{ij}(k) = k$  for all  $k \neq i, j$ . If  $\mathbf{r} = (r_1, \dots, r_L)$ , then

$$\mathbf{t}_{ij} * \mathbf{r} = (r_1, \dots, r_{i-1}, r_j, r_{i+1}, \dots, r_{j-1}, r_i, r_{j+1}, \dots, r_L). \quad (41)$$

If  $|i - j| = 1$ , then  $\mathbf{t}_{ij}$  is called an *adjacent transposition*. Unlike factorization of permutations into disjoint cycles, the factorization of permutations into adjacent transpositions (and, hence, into transpositions) is not unique, although the minimal number of factors is. For example,  $321 = (12)(23)(12) = (23)(12)(23)$ .

**Definition 11** Let  $\mathbf{r}, \mathbf{s} \in \text{Sym}(L)$ . The Cayley (resp. Kendall) distance between  $\mathbf{r}$  and  $\mathbf{s}$ , denoted by  $d_C(\mathbf{r}, \mathbf{s})$  (resp.  $d_K(\mathbf{r}, \mathbf{s})$ ), is defined as the minimum number of transpositions (resp. adjacent transpositions) needed to transform  $\mathbf{r}$  into  $\mathbf{s}$ .

The proof that  $d_C$  and  $d_K$  are distances in the axiomatic sense is straightforward and can be found (using graph-theoretical arguments for the triangular inequality) in Amigó and Dale<sup>16</sup>.

Figure 1 shows the adjacency graph of  $\text{Sym}(4)$ , i.e., each node corresponds to a permutation  $\mathbf{r} \in \text{Sym}(4)$  and two nodes are connected by a link if they differ by an adjacent transposition. So the distance  $d_K(\mathbf{r}, \mathbf{s})$  is the length (number of links) of the shortest path between  $\mathbf{r}$  and  $\mathbf{s}$ . For a 3D rendering of the adjacency group of  $\text{Sym}(4)$ , see the permutohedron<sup>65</sup>. The adjacency graph of  $\text{Sym}(3)$  is just a cycle<sup>16</sup>.

The distances  $d_C(\mathbf{r}, \mathbf{s})$  and  $d_K(\mathbf{r}, \mathbf{s})$  can be calculated using the following formulas, both involving the transcript  $T_{\mathbf{r}, \mathbf{s}} = \mathbf{s} * \mathbf{r}^{-1}$ . In view of Definition 11, it is not surprising that the transcript  $T_{\mathbf{r}, \mathbf{s}}$  is related to  $d_C(\mathbf{r}, \mathbf{s})$  and  $d_K(\mathbf{r}, \mathbf{s})$ : By equation (10),  $T_{\mathbf{r}, \mathbf{s}} * \mathbf{r} = \mathbf{s}$ , so  $T_{\mathbf{r}, \mathbf{s}}$  is the element of  $\mathcal{G}$  that transforms  $\mathbf{r}$  into  $\mathbf{s}$ .

**Proposition 12** (a) Let  $\mathbf{u} = (u_1, \dots, u_L) \in \text{Sym}(L)$  and  $C(\mathbf{u})$  be the number of cycles (including 1-cycles) in the cycle factorization of the permutation  $\mathbf{u}$ . Then,

$$d_C(\mathbf{r}, \mathbf{s}) = L - C(\mathbf{s} * \mathbf{r}^{-1}) = L - C(T_{\mathbf{r}, \mathbf{s}}) \quad (42)$$

for all  $\mathbf{r}, \mathbf{s} \in \text{Sym}(L)$ .

(b) Let  $I(\mathbf{u})$  be the number of inversions in the permutation  $\mathbf{u}$ , i.e., the number of ordered pairs  $(u_i, u_j)$ ,  $1 \leq i < j \leq L$ , such that  $u_i > u_j$ . Then

$$d_K(\mathbf{r}, \mathbf{s}) = I(\mathbf{s} * \mathbf{r}^{-1}) = I(T_{\mathbf{r}, \mathbf{s}}) \quad (43)$$

for all  $\mathbf{r}, \mathbf{s} \in \text{Sym}(L)$ .

Of course,  $d_C(\mathbf{r}, \mathbf{s}) = d_C(\mathbf{s}, \mathbf{r})$  amounts to  $C(T_{\mathbf{r}, \mathbf{s}}) = C(T_{\mathbf{s}, \mathbf{r}})$ , and  $d_K(\mathbf{r}, \mathbf{s}) = d_K(\mathbf{s}, \mathbf{r})$  to  $I(T_{\mathbf{r}, \mathbf{s}}) = I(T_{\mathbf{s}, \mathbf{r}})$ . By definition,

$$d_C(\mathbf{r}, \mathbf{s}) \leq d_K(\mathbf{r}, \mathbf{s}). \quad (44)$$

Furthermore, from equations (42) and (43) it follows

$$d_C(\mathbf{r}, \mathbf{s}) \in \{0, 1, \dots, d_{C, \max} := L - 1\}, \quad (45)$$

and

$$d_K(\mathbf{r}, \mathbf{s}) \in \left\{ 0, 1, \dots, d_{K, \max} := \frac{L(L-1)}{2} \right\}, \quad (46)$$

Therefore,  $d_{K, \max} > d_{C, \max}$ , except for  $L = 2$ , which generally makes  $d_K$  a better choice in applications.

An important property of  $d_C$  and  $d_K$  is *right-invariance*: Since

$$T_{\mathbf{e}, \mathbf{s} * \mathbf{r}^{-1}} = \mathbf{s} * \mathbf{r}^{-1} = T_{\mathbf{r}, \mathbf{s}}, \quad (47)$$

we derive from equation (42)-(43) that

$$d_{C,K}(\mathbf{r}, \mathbf{s}) = d_{C,K}(\mathbf{e}, \mathbf{s} * \mathbf{r}^{-1}), \quad (48)$$

where  $\mathbf{e} = 12 \dots L$  is the identity permutation and, here and below, we use the shorthand  $d_{C,K}$  to refer to both the Cayley and Kendall distances. Define the usual norm

$$\|\mathbf{r}\|_{C,K} := d_{C,K}(\mathbf{e}, \mathbf{r}) \quad (49)$$

in the metric spaces  $(\text{Sym}(L), d_{C,K})$  to write equation (48) in the appealing form

$$d_{C,K}(\mathbf{r}, \mathbf{s}) = \|T_{\mathbf{r}, \mathbf{s}}\|_{C,K}. \quad (50)$$

According to equation (48), all possible distances  $d_{C,K}(\mathbf{r}, \mathbf{s})$  appear in the  $\mathbf{e}$ -row (i.e.,  $(d_{C,K}(\mathbf{e}, \mathbf{u}))_{\mathbf{u} \in \text{Sym}(L)}$ ) of the distance matrix  $(d_{C,K}(\mathbf{r}, \mathbf{s}))_{\mathbf{r}, \mathbf{s} \in \text{Sym}(L)}$ .

**Example 13** The Cayley and Kendall distance matrices for the group  $\text{Sym}(3)$ , equation (7), are the following:

$d_C(\mathbf{r}, \mathbf{s})$	123	132	213	231	312	321
123	0	1	1	2	2	1
132	1	0	2	1	1	2
213	1	2	0	1	1	2
231	2	1	1	0	2	1
312	2	1	1	2	0	1
321	1	2	2	1	1	0

(51)

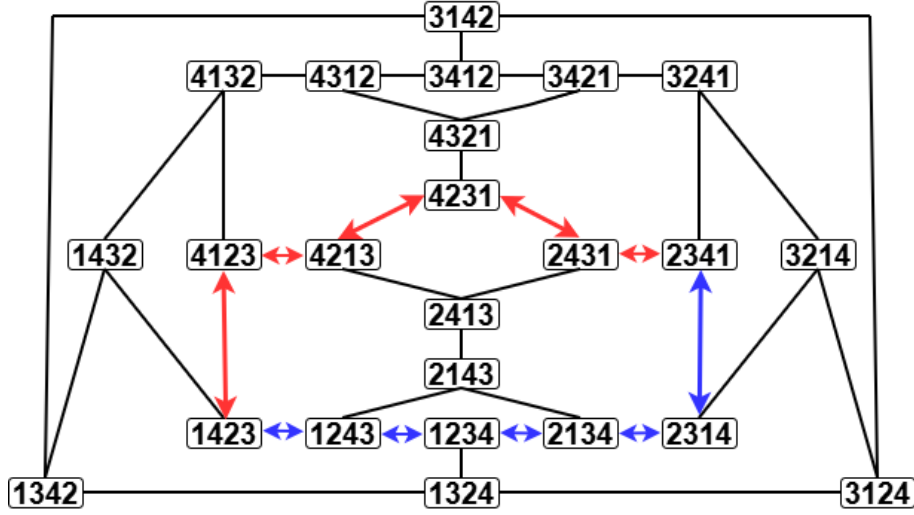


FIG. 1. Adjacency graph of  $\text{Sym}(4)$ . A link between two permutations means that the Kendall distance (minimum number of adjacent transpositions that transforms one of them into the other) is 1. The figure highlights two (out of five) shortest paths between the permutations 1423 and 2341, marked with bidirectional arrows (in blue and red online), showing that  $d_K(1423, 2341) = 5$ .

and

$d_K(\mathbf{r}, \mathbf{s})$	123	132	213	231	312	321
123	0	1	1	2	2	3
132	1	0	2	3	1	2
213	1	2	0	1	3	2
231	2	3	1	0	2	1
312	2	1	3	2	0	1
321	3	2	2	1	1	0

(52)

As shown in equations (44)-(46),  $d_C(\mathbf{r}, \mathbf{s}) \leq d_K(\mathbf{r}, \mathbf{s})$  for all  $\mathbf{r}, \mathbf{s} \in \text{Sym}(3)$ ,  $d_C(\mathbf{r}, \mathbf{s}) \in \{0, 1, 2\}$ , and  $d_K(\mathbf{r}, \mathbf{s}) \in \{0, 1, 2, 3\}$ . All these possible distances appear in the first row (row 123) of the corresponding distance matrix. The distance matrices for  $\text{Sym}(4)$  can be found in the Appendix of Amigó and Dale<sup>16</sup>.

Empirical probability distributions of the distances

$$\text{dist}(\mathbf{r}_t, \mathbf{s}_t) := d_{C,K}(\mathbf{r}_t, \mathbf{s}_t)_{1 \leq t \leq N-L+1} \quad (53)$$

have been used<sup>16</sup> to characterize generalized synchronization in a drive-response system composed of two Hénon maps, which has two different synchronization regimes: weak and strong. To this end, the first components of the driver and responder were discretized with ordinal patterns of lengths  $L = 4, 5$ , providing the time series  $\alpha = (\mathbf{r}_t)_{1 \leq t \leq N}$  and  $\beta = (\mathbf{s}_t)_{1 \leq t \leq N}$ . The results showed that weak synchronization characterizes by forbidden short distances, while strong synchronization does by forbidden long distances. Since  $d_K$  has a greater range than  $d_C$  for the same  $L \geq 3$ , the former has greater differentiating power than the latter.

More generally, sliding windows  $\mathbf{r}_t^W = (\mathbf{r}_t, \mathbf{r}_{t+1}, \dots, \mathbf{r}_{t+W-1})$  and  $\mathbf{s}_t^W = (\mathbf{s}_t, \mathbf{s}_{t+1}, \dots, \mathbf{s}_{t+W-1})$  of size  $W \geq 2$  have also been used<sup>16</sup> for characterizing generalized synchronization in the

above drive-response system, their similarity being measured by the  $l_p$ -distances

$$\text{dist}_p(\mathbf{r}_t^W, \mathbf{s}_t^W) = \left( \sum_{k=0}^{W-1} \text{dist}(\mathbf{r}_{t+k}, \mathbf{s}_{t+k})^p \right)^{1/p} \quad (54)$$

for  $1 \leq p < \infty$ , and

$$\text{dist}_\infty(\mathbf{r}_t^W, \mathbf{s}_t^W) = \max \{ \text{dist}(\mathbf{r}_{t+k}, \mathbf{s}_{t+k}) : 0 \leq k \leq W-1 \}. \quad (55)$$

In this case, one ends up with an integer (for  $p = 1, \infty$ ) or real (for  $1 < p < \infty$ ) sequence

$$(\text{dist}_p(\mathbf{r}_t^W, \mathbf{s}_t^W))_{1 \leq t \leq N-W+1} \quad (56)$$

that contains metric information about the time series  $(\mathbf{r}_t)$  and  $(\mathbf{s}_t)$ . Distances  $\text{dist}_p$  with smaller parameters  $p$  (say, the Manhattan distance  $\text{dist}_1$  and the Euclidean distance  $\text{dist}_2$ ) have greater differentiating power due to the monotony property of the  $p$ -norms ( $\|\cdot\|_p \geq \|\cdot\|_{p'}$  for  $1 \leq p \leq p' \leq \infty$ ). The results supported the results obtained with simultaneous ordinal patterns ( $W = 1$ ), equation (53).

## F. Distances in general groups via permutations

Given a group  $\mathcal{G}$ , a finite set  $S = \{s_1, \dots, s_n\} \subset \mathcal{G}$  is a *generating set* (or generator) of  $\mathcal{G}$  if every  $a \in \mathcal{G}$  can be written as a finite product of elements of  $S$  and their inverses. The distance (or *word metric*)  $d_S(a, b)$  between two elements  $a, b \in \mathcal{G}$  is defined<sup>12</sup> as the minimum number of elements from the generating set  $S$  needed to transform  $a$  into  $b$ . In particular, if  $\mathcal{G} = \text{Sym}(L)$ , then the Cayley distance  $d_C(\mathbf{r}, \mathbf{s})$  is the distance  $d_S$  with respect to the generating set of all transpositions, while

the Kendall distance  $d_K(\mathbf{r}, \mathbf{s})$  is the distance  $d_S$  with respect to the generating set of all adjacent transpositions.

For groups  $\mathcal{G}$  other than  $\text{Sym}(L)$ , a different approach was proposed in Amigó and Dale<sup>16</sup> which dispenses with generating sets and, hence, with the search for minimal factorizations of transcripts using generating elements. This method is based on Cayley's Theorem (Theorem 5), which allows embedding any group  $(\mathcal{G}, \cdot)$  into the symmetric group  $\text{Sym}(\mathcal{G})$ .

**Definition 14** Let  $\Phi: \mathcal{G} \rightarrow \text{Sym}(\mathcal{G})$  be the Cayley embedding for a finite group  $(\mathcal{G}, \cdot)$ . Then,  $D_{C,K}^{(\Phi)}$  is the distance in  $\mathcal{G}$  defined as

$$D_{C,K}^{(\Phi)}(a, b) = d_{C,K}(\Phi(a), \Phi(b)) \quad (57)$$

for all  $a, b \in \mathcal{G}$ .

Hence,  $D_{C,K}^{(\Phi)}$  has the same properties as  $d_{C,K}$ . In particular:

- For  $a, b \in \mathcal{G}$ ,

$$D_C^{(\Phi)}(a, b) \leq D_K^{(\Phi)}(a, b), \quad (58)$$

where

$$D_C^{(\Phi)}(a, b) \in \left\{ 0, 1, \dots, D_{C,\max}^{(\Phi)} := |\mathcal{G}| - 1 \right\}, \quad (59)$$

and

$$D_K^{(\Phi)}(a, b) \in \left\{ 0, 1, \dots, D_{K,\max}^{(\Phi)} := \frac{|\mathcal{G}|(|\mathcal{G}| - 1)}{2} \right\}. \quad (60)$$

- If  $e$  is the identity of  $\mathcal{G}$ , then

$$D_{C,K}^{(\Phi)}(a, b) = D_{C,K}^{(\Phi)}(e, T_{a,b}). \quad (61)$$

In the case  $\mathcal{G} = \text{Sym}(L)$ , Section V E, the distances  $d_{C,K}(\mathbf{r}, \mathbf{s})$  take on all integer values ranging from 0 to their respective maxima:  $d_{C,\max} = L - 1$  (equation (45)), and  $d_{K,\max} = L(L - 1)/2$  (equation (46)). However, this does not happen with  $D_{C,K}^{(\Phi)}(a, b)$  because  $\Phi(\mathcal{G})$  is a subgroup of cardinality  $|\mathcal{G}|$  of the group  $\text{Sym}(\mathcal{G})$ , whose cardinality is  $|\mathcal{G}|!$ , so not all possible distances can be realized (unless  $|\mathcal{G}| = 2$ ). We call “the gaps in  $D_{C,K}^{(\Phi)}$ ” the values in  $\{0, 1, \dots, D_{C,K,\max}^{(\Phi)}\}$  missing from the distance matrix  $(D_{C,K}^{(\Phi)}(a, b))_{a,b \in \mathcal{G}}$ ; otherwise, they are called allowed or admissible distances. By equation (61), the admissible distances for  $D_{C,K}^{(\Phi)}$  can be read in the row  $(D_{C,K}^{(\Phi)}(e, c))_{c \in \mathcal{G}}$  of the distance matrix. Hence, the maximum number of admissible distances for  $D_{C,K}^{(\Phi)}$  is  $|\mathcal{G}|$ .

According to Theorem 8, the Cayley embedding  $\Phi: \mathcal{G} \rightarrow \text{Sym}(\mathcal{G})$  can be implemented via the left translations  $a \mapsto \tilde{T}_a := \tilde{T}(a, \cdot)$ , where  $\tilde{T}(a, b) = a^{-1} \cdot b$  is the conjugate transcription mapping, equation (11). In this case, we write  $D_{C,K}^{(\tilde{T})}$  instead of  $D_{C,K}^{(\Phi)}$  to specify that the embedding  $\Phi$  is implemented by conjugate transcripts.

**Example 15** Consider again the Klein four-group  $\mathcal{K}$ , Example 9, and the Cayley isomorphism  $\Phi(r) = \tilde{T}_r: \mathcal{K} \rightarrow \text{Sym}(4)$ . To calculate the Kendall distances  $D_K^{(\tilde{T})}(r, s) = d_K(\tilde{T}_r, \tilde{T}_s)$ , we are going to take advantage of the adjacency graph of the embedding symmetric group  $\text{Sym}(4)$ , Figure 1. To this end, we use the encoding (19), locate the isomorphic copies

$$\tilde{T}_e = 1234, \tilde{T}_a = 2143, \tilde{T}_b = 3412, \tilde{T}_c = 4321,$$

(see equation (20)) in Figure 1, and read there the distances between them. The result is

$D_K^{(\tilde{T})}$	$e$	$a$	$b$	$c$
$e$	0	2	4	6
$a$	2	0	6	4
$b$	4	6	0	2
$c$	6	4	2	0

(62)

As noted before, all allowed distances can be read in the row corresponding to  $\Phi(e) = \tilde{T}_e$  of the distance matrix. Since  $D_K^{(\tilde{T})}(r, s) \in \{0, 1, \dots, 6\}$  according to equation (60), only the even values (including 0) are allowed for  $D_K^{(\tilde{T})}$ . It is interesting that the nodes 1234, 2143, 3412, and 4321 are located on the central axis of the  $\text{Sym}(4)$  adjacency graph, symmetrically positioned with respect to the center of the graph.

## VI. NUMERICAL SIMULATIONS

In this section we are going to test numerically the performance of some representative tools from Section V in generalized synchronization detection. To this end we resort to the same model used in Amigó and Dale<sup>16</sup> where, instead, the probability distributions of some Kendall and  $l_p$ -distances were analysed. The model is composed of two unidirectionally coupled, non-identical Hénon systems<sup>66</sup>. The equations of the driver  $X$  are

$$\begin{cases} x_{t+1}^{(1)} = 1.4 - (x_t^{(1)})^2 + 0.1x_t^{(2)} \\ x_{t+1}^{(2)} = x_t^{(1)} \end{cases} \quad (63)$$

and the equations of the responder  $Y$  are

$$\begin{cases} y_{t+1}^{(1)} = 1.4 - [Cx_t^{(1)} + (1 - C)y_t^{(1)}]y_t^{(1)} + 0.3y_t^{(2)} \\ y_{t+1}^{(2)} = y_t^{(1)} \end{cases} \quad (64)$$

where  $C > 0$  is the *coupling constant* or *strength*. The reason for selecting this model here again is two-fold: (i) it has *generalized synchronization*<sup>67–69</sup> in the parametric interval  $0.50 \lesssim C \lesssim 0.60$  and for  $C \gtrsim 0.90$  (Figure 3 of Amigó et al.<sup>70</sup>), and (ii) we can compare some of our results here with the results obtained there by other means and cross-interpret each result with the help of the others. We will refer to the generalized synchronization of the system (63)-(64) for  $0.50 \lesssim C \lesssim 0.60$  and  $C \gtrsim 0.90$  as “weak” and “strong” synchronization, respectively.

For a given coupling constant  $C$ , let  $\mathbf{x} = (x_t^{(1)})_{1 \leq t \leq N}$  and  $\mathbf{y} = (y_t^{(1)})_{1 \leq t \leq N}$  be two stationary time series of length  $N =$

10,000 composed of the first components of the states  $x_t = (x_t^{(1)}, x_t^{(2)})$  of the driver and  $y_t = (y_t^{(1)}, y_t^{(2)})$  of the responder, respectively, and obtained with seeds (0,0.9) and (0.75,0) after discarding an initial transient. Let  $\alpha = (\mathbf{r}_t)_{1 \leq t \leq N-L+1}$  and  $\beta = (\mathbf{s}_t)_{1 \leq t \leq N-L+1}$  be the algebraic representations of  $x$  and  $y$  using ordinal patterns of length  $L = 3$ , and  $T_{\alpha,\beta} = (\mathbf{t}_t)_{1 \leq t \leq N-L+1} = (\mathbf{s}_t * \mathbf{r}_t^{-1})_{1 \leq t \leq N-L+1}$  the corresponding transcript time series. The values chosen for the coupling strength are  $0 \leq C \leq 1.2$  with  $\Delta C = 0.05$ . For computer codes to calculate ordinal patterns and tools, see Unakafova and Keller<sup>19</sup>, Berger et al.<sup>71</sup>, and Pessa and Ribeiro<sup>72</sup>.

### A. Results with the entropy-complexity plane

Let  $P_\tau$  be the transcript probability distribution obtained from the time series  $T_{\alpha,\beta}$  with coupling constant  $C$ . Figure 2 shows the values of the normalized Shannon entropy  $h(P_\tau)$  (equation (27) with  $\Lambda = 0$  and  $|\mathcal{G}| = |\text{Sym}(3)| = 6$ ) and the statistical complexity

$$\text{SC}(P_\tau) = D_{JS}(P_\tau \| U)h(P_\tau) \quad (65)$$

(equation (31)) on the entropy-complexity plane<sup>55</sup> for  $C = 0.05k$  and  $0 \leq k \leq 24$ . Here  $U$  is the uniform distribution over 6 events. We use base 2 logarithms so that  $0 \leq \text{SC}(P_\tau) \leq 1$ .

The dashed circle in the lower left of Figure 2 encloses the coupled systems with (left to right)  $C = 0.95, 1.00, 0.85, 0.90, 1.05, 1.10, 1.15$ , and  $1.20$  (where  $C = 0.85, 0.90$  overlap, as well as  $C = 1.15, 1.20$ ), i.e., all strongly synchronized systems ( $C \geq 0.90$ ) and one nearly strongly synchronized system ( $C = 0.85$ ).

On the other hand, the dashed square in the upper center of Figure 2 encompasses the coupled systems with coupling constants (left to right)  $C = 0.55, 0.65, 0.45, 0.40, 0.50$  and  $0.60$ , i.e., all weakly synchronized systems ( $0.50 \leq C \leq 0.60$ ) and three nearly weakly synchronized system ( $C = 0.40, 0.45, 0.65$ ).

Points located in the lower right corner of the entropy-complexity plane correspond to systems with small coupling strengths.

The main conclusions from Figure 2 can be summarized as follows.

- All transcript time series generated by strongly synchronized systems (left cluster) have a lower complexity than the transcript time series generated by weakly and nearly weakly synchronized systems (upper cluster). The lowest statistical complexities (lower right corner) correspond to weakly coupled systems.
- Also, transcript time series corresponding to weak synchronization have a greater entropy than those corresponding to strong synchronization. The transcript time series with the highest entropies correspond to weakly coupled systems.

Therefore, the entropy-complexity plane can discriminate strong from weak synchronization in the drive-response

model (63)-(64) parameterized by the coupling constant  $C$ . The systems are roughly located along a parabola, the left and right branches corresponding to systems with strong and weak couplings, respectively. Weakly synchronized and nearly weakly synchronized systems are located around the top of the parabola. However, while the points corresponding to strong synchronization are closely grouped, the points corresponding to weak synchronization are more scattered and mixed with points corresponding to nearly, but not strictly belonging to, weak synchronization. Therefore, the entropy-complexity plane is an accurate clustering tool for strong synchronization but not for weak synchronization. The joint asymptotic probability distribution of entropy and complexity has been studied by Silbernagel and Weiß<sup>73</sup>.

### B. Results with transcript mutual information

Given the two coupled systems  $X$  and  $Y$  in equations (63)-(64), and the observations  $x = (x_t^{(1)})_{1 \leq t \leq N}$  and  $y = (y_t^{(1)})_{1 \leq t \leq N}$ , the symbolic transfer entropy<sup>58</sup>

$$\text{TE}_{\alpha \rightarrow \beta}(\Lambda) = I(\mathbf{s}_{t+\Lambda}; \mathbf{r}_t | \mathbf{s}_t) \quad (66)$$

is a measure of the information transferred from  $X$  to  $Y$  based on the ordinal representations  $\alpha = (\mathbf{r}_t)_{1 \leq t \leq N-L+1}$  and  $\beta = (\mathbf{s}_t)_{1 \leq t \leq N-L+1}$  of  $x$  and  $y$ , where here  $\mathbf{r}_t, \mathbf{s}_t \in \text{Sym}(3)$ .

As explained in Section V C, the transcript mutual information

$$\text{TMI}_{\alpha \rightarrow \beta}(\Lambda) = I(T_{\mathbf{s}_{t+\Lambda}, \mathbf{s}_t}; T_{\mathbf{r}_t, \mathbf{s}_t}) \quad (67)$$

coincides with  $\text{TE}_{\alpha \rightarrow \beta}(\Lambda)$  when two conditions are met: (i)  $H(\mathbf{s}_t) \leq H(\mathbf{r}_t)$  and (ii)  $C(\beta_\Lambda, \beta, \alpha) = 0$ , where  $C(\cdot)$  is the coupling complexity coefficient of dimension 3 defined in equation (33). Although condition (ii) is often only approximately met, numerical simulations and analysis with real data indicate that, in general,  $C(\beta_\Lambda, \beta, \alpha) \rightarrow 0$  and, hence,  $\text{TMI}_{\alpha \rightarrow \beta}(\Lambda) \rightarrow \text{TE}_{\alpha \rightarrow \beta}(\Lambda)$  as the time lag  $T$  increases.

On the other hand, the possibility of calculating or estimating a 3-dimensional information directionality indicator (symbolic transfer entropy) with a 2-dimensional quantity (transcript mutual information) is a very useful result in practice, where time series used to be short and probabilities have to be estimated by frequencies. Considering that, when determining the information directionality, we are usually only interested in the sign of  $\text{TE}_{\alpha \rightarrow \beta}(\Lambda)$ , the approximation error  $\varepsilon = |\text{TE}_{\alpha \rightarrow \beta}(\Lambda) - \text{TMI}_{\alpha \rightarrow \beta}(\Lambda)|$  is inconsequential as long as  $\text{TE}_{\alpha \rightarrow \beta}(\Lambda)$  and  $\text{TMI}_{\alpha \rightarrow \beta}(\Lambda)$  have the same sign, which translates into the assumption  $\varepsilon < |\text{TE}_{\alpha \rightarrow \beta}(\Lambda)|$ .

Figure 3 shows  $\text{TE}_{\alpha \rightarrow \beta} := \text{TE}_{\alpha \rightarrow \beta}(1)$  and  $\text{TMI}_{\alpha \rightarrow \beta} := \text{TMI}_{\alpha \rightarrow \beta}(1)$  as functions of the coupling strength  $C$  for time lags  $T = 1$  (left panel) and  $T = 5$  (right panel). As expected, the approximation error  $\varepsilon$  is lower for  $T = 5$ , in particular,  $\text{TMI}_{\alpha \rightarrow \beta}(1) = 0$  for  $C = 0$  in that case. The main conclusions from Figure 3 can be summarized as follows.

- The signs of  $\text{TE}_{\alpha \rightarrow \beta}$  and  $\text{TMI}_{\alpha \rightarrow \beta}$  coincide and are positive for  $C > 0$ , as they should. As shown in the right

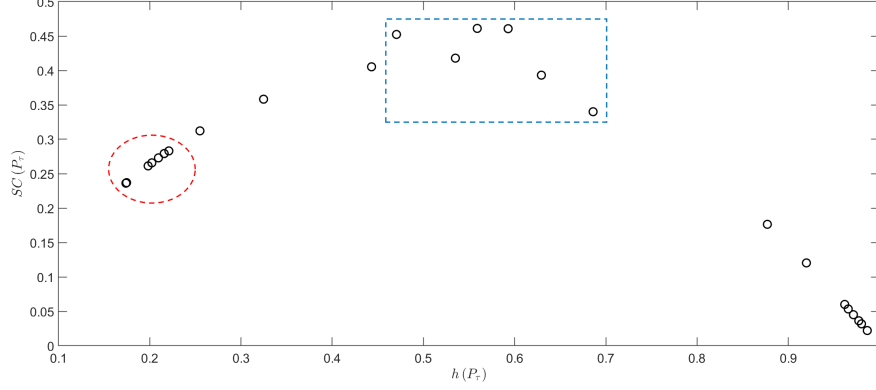


FIG. 2. Entropy-complexity plane  $h(P_\tau) \times SC(P_\tau)$  for the Hénon-Hénon system (63)-(64). Each point on the plane corresponds to a time series of length-3 transcripts, obtained with a given coupling strength. All points corresponding to strong synchronization ( $C \gtrsim 0.9$ ) cluster inside the dashed circle in the lower left of the plane. Points corresponding to weak synchronization ( $0.50 \lesssim C \lesssim 0.60$ ) and nearly weak synchronization ( $C = 0.40, 0.45, 0.65$ ) are distributed inside the dashed square in the upper center of the plane.

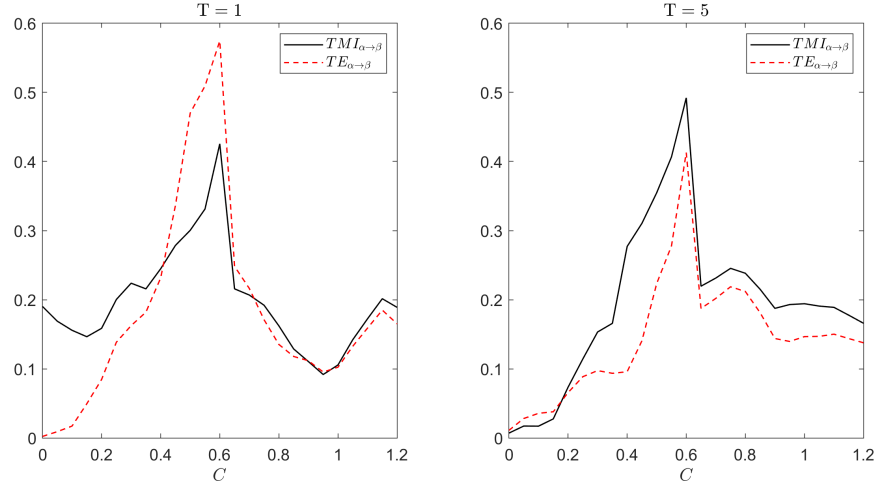


FIG. 3. Symbolic transfer entropy  $TE_{\alpha \rightarrow \beta}(1) = I(\mathbf{s}_{t+1}; \mathbf{r}_t | \mathbf{s}_t) =: TE_{\alpha \rightarrow \beta}$  and transcript mutual information  $TMI_{\alpha \rightarrow \beta}(1) = (T_{\mathbf{s}_{t+1}, \mathbf{s}_t}; T_{\mathbf{r}_t, \mathbf{s}_t}) =: TMI_{\alpha \rightarrow \beta}$  as functions of the coupling strength  $C$  for time lags  $T = 1$  (left panel) and  $T = 5$  (right panel). The positivity of the two directionality indicators for the coupling delay  $\Lambda = 1$  in both panels suggests that the process  $\alpha$  is driving the process  $\beta$ . Also in both panels, the most visible feature of each curve is its global maximum at weak synchronization ( $C \simeq 0.60$ ), while strong synchronization is not particularly signalized.

panel, the deviation of  $TMI_{\alpha \rightarrow \beta}$  from  $TE_{\alpha \rightarrow \beta}$ , especially for  $C \leq 0.60$ , can be reduced by taking larger time lags in the time series  $x$  and  $y$ .

- Again, we observe a kind of complementary behavior regarding the two synchronization states. For weak synchronization, both directionality indicators have an absolute maximum, while their magnitudes in the strong synchronization state are comparable to other dynamics with small couplings.

We conclude that the performance of the transcript mutual information  $TMI_{\alpha \rightarrow \beta}$  is satisfactory to detect the driver, but unsatisfactory when it comes to detecting generalized syn-

chronization.

### C. Results with transcript order classes

In Amigó and Dale<sup>16</sup>, we found a kind of correspondent behavior of the forbidden distances with respect to the weak and strong synchronizations regimes, namely: for  $\mathbf{r}, \mathbf{s} \in \text{Sym}(L)$  and  $L = 4, 5$ , short distances ( $d_K(\mathbf{r}, \mathbf{s}) = 0, 1, \dots$ ) are forbidden in the weak regime ( $C = 0.55$ ), whereas long distances ( $d_K(\mathbf{r}, \mathbf{s}) = d_{K, \max}, d_{K, \max} - 1, \dots$ ) are forbidden in the strong regime ( $C = 1.10$ ). This correspondence seems to be reflected also in Figure 4(a), this time with the probabilities of the tran-

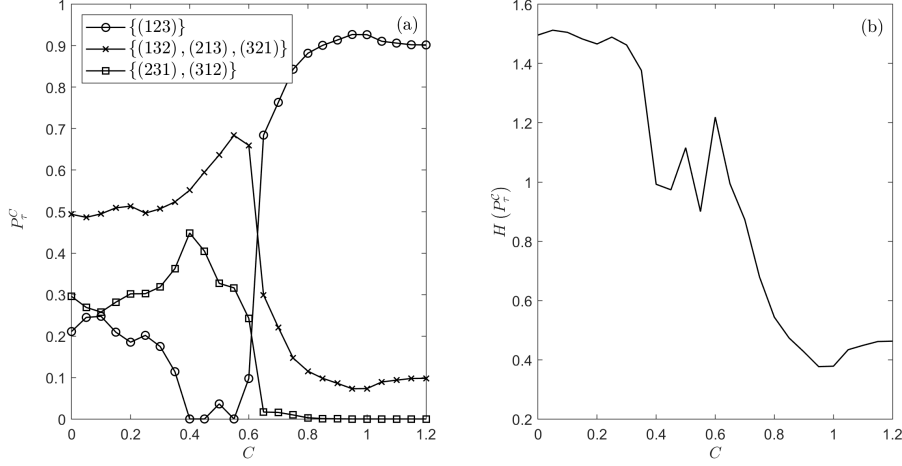


FIG. 4. (a) Probabilities of the transcript order classes (see inset) as function of the coupling strength  $C$ . The probabilities of the lowest and greatest order classes,  $\mathcal{C}_1$  and  $\mathcal{C}_3$ , at the two synchronization regimes are correlative in the following sense:  $\mathcal{C}_1 = \emptyset$  for weak synchronization while  $\mathcal{C}_3 = \emptyset$  for strong synchronization. (b) Entropy of the order class probability distribution  $P_C^c$ , equation (39). In this case weak synchronization is characterized by a local minimum at  $C = 0.55$ , while strong synchronization is characterized by an absolute minimum at  $C = 1$ .

script order classes of the group  $\text{Sym}(3)$ :

$$\mathcal{C}_1 = \{123\}, \mathcal{C}_2 = \{132, 213, 321\}, \mathcal{C}_3 = \{231, 312\}. \quad (68)$$

To be more specific:

- For  $C = 0.40, 0.45, 0.55$ , the transcript  $\mathbf{t}_t = 123$  is forbidden (that is,  $\mathcal{C}_1 = \{123\} = \emptyset$ ), which means that, for weakly synchronized (and nearly synchronized) systems,  $\mathbf{s}_t \neq \mathbf{r}_t$  for all  $t \geq 0$ , i.e., the ordinal 3-patterns of the driver and responder never coincide. For  $C = 0.50, 0.60$ , the probability of  $\mathbf{t}_t = 123$  is not strictly 0 but very small.
- For  $C \gtrsim 0.85$ ,  $p_\tau(123) \gtrsim 0.9$ , meaning that, for strongly synchronized systems, the ordinal 3-patterns of the driver and responder coincide more than 90% of the time. Furthermore, the transcript 321 is forbidden in the same parametric interval (not shown), hence, if  $\mathbf{r}_t = k_1 k_2 k_3$  then  $\mathbf{s}_t \neq k_3 k_2 k_1$ .
- For  $C \geq 0.95$ , the order class  $\mathcal{C}_3 = \{231, 312\}$  is empty, which means that, in the regime of strong synchronization,  $\mathbf{r}_t \in \mathcal{C}_1$  implies  $\mathbf{s}_t \in \mathcal{C}_1 \cup \mathcal{C}_2$ , (ii)  $\mathbf{r}_t \in \mathcal{C}_2$  implies  $\mathbf{s}_t \in \mathcal{C}_1 \cup \mathcal{C}_3$ , and (iii)  $\mathbf{r}_t \in \mathcal{C}_3$  implies  $\mathbf{s}_t \in \mathcal{C}_2$ .

In sum, weak and strong generalized synchronization impose restrictions on the joint probabilities  $p(\mathbf{r}_t, \mathbf{s}_t)$  that can be detected at the coarse scale of transcript order classes of  $\text{Sym}(3)$ .

The entropy of the probability distribution of the transcript order classes given in Figure 4(a) is depicted in Figure 4(b). As in Figure 2, we see again that strong synchronization is characterized by the global lowest transcript entropy, while transcript entropy has a local minimum at weak synchronization.

**Remark 16** Let us also point out that there is a direct correspondence between transcript order classes and Cayley distance when  $\mathcal{G} = \text{Sym}(3)$ . According to equation (68) and the distance matrix for  $d_C(\mathbf{r}, \mathbf{s})$  in equation (51), it holds

$$d_C(\mathbf{r}, \mathbf{s}) = d_C(\mathbf{e}, T_{\mathbf{r}, \mathbf{s}}) = n \in \{0, 1, 2\} \Leftrightarrow T_{\mathbf{r}, \mathbf{s}} \in \mathcal{C}_{n+1}, \quad (69)$$

where  $\mathbf{e} = 123$ , hence

$$\text{ord}(T_{\mathbf{r}, \mathbf{s}}) - 1 = d_C(\mathbf{r}, \mathbf{s}). \quad (70)$$

In other words, the integer  $\text{ord}(T_{\mathbf{r}, \mathbf{s}}) - 1$  is actually a distance for the group  $\text{Sym}(3)$ , namely, the Cayley distance between  $\mathbf{r}$  and  $\mathbf{s}$ .

For the Kendall distance  $d_K(\mathbf{r}, \mathbf{s})$ , the identification (69) is also correct except for  $T_{\mathbf{r}, \mathbf{s}} = 321$  (see equation (52)). This explains the correlation between forbidden distances and empty order classes mentioned above, which is exact in the case of Cayley distances.

#### D. Results with algebraic and entropic distances

Finally, we consider two distances between the symbolic time series  $\alpha = (\mathbf{r}_t)_{1 \leq t \leq N-L+1}$  and  $\beta = (\mathbf{s}_t)_{1 \leq t \leq N-L+1}$  for each coupling constant  $0 < C \leq 1.2$ ,  $\Delta C = 0.05$ . First, we take the mean value over time of the sequence of normalized Kendall distances  $d_K(\mathbf{r}_t, \mathbf{s}_t)$ ,

$$(d_K(\mathbf{r}_t, \mathbf{s}_t) / d_{K, \max})_{1 \leq t \leq N-2} = (\|T_{\mathbf{r}_t, \mathbf{s}_t}\|_K / 3)_{1 \leq t \leq N-2},$$

to obtain the *similarity distance*

$$\delta_K(\alpha, \beta) = \frac{1}{3(N-2)} \sum_{t=1}^{N-2} \|T_{\mathbf{r}_t, \mathbf{s}_t}\|_K \quad (71)$$

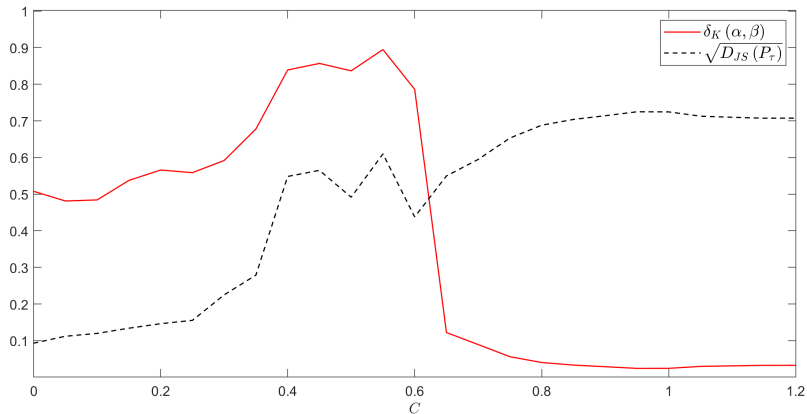


FIG. 5. The transcript-based similarity distance  $\delta_K(\alpha, \beta)$  and the entropy-based, normalized distance  $D_{JS}(P_\tau)^{1/2}$  versus the coupling strength  $C$ . The metric  $\delta(\alpha, \beta)$  measures the average Kendall distance  $d_K(\mathbf{r}_t, \mathbf{s}_t)$  between simultaneous ordinal patterns of the driver and responder;  $D_{JS}(P_\tau)^{1/2}$  measures the similarity between the transcript probability distributions  $P_\tau$  and the uniform distribution  $U$ . In doing so,  $\delta_K(\alpha, \beta)$  achieves a global maximum at weak synchronization ( $C \simeq 0.55$ ) and a flat global minimum at strong synchronization ( $C \gtrsim 1.0$ ), which is a clear signal in both cases.

between  $\alpha$  and  $\beta$  for each  $C$ . So,  $\delta_K(\alpha, \beta)$  measures similarity in the following sense: the smaller (resp. greater)  $\delta_K(\alpha, \beta)$  is, the more similar (resp. dissimilar)  $\alpha$  and  $\beta$  will be, meaning that the symbols of the time series  $\alpha$  and  $\beta$  will be closer (resp. more distant) on average, where distance is measured by  $d_K$ .

To compare the performance of the transcript-based metric  $\delta_K(\alpha, \beta)$  with other metrics, we have selected the square root of the normalized Jensen-Shannon divergence,  $D_{JS}(P_\tau)^{1/2}$ , equation (65), which, according to Section VB, is a distance in axiomatic sense between the probability distribution  $P_\tau$  and the uniform distribution  $U$ . Therefore, the smaller (resp. greater)  $D_{JS}(P_\tau)^{1/2}$  is, the more similar (resp. dissimilar)  $P_\tau$  and  $U$  will be. Since  $C = 0$  corresponds to the driver and responder being independent (uncoupled), we expect that  $D_{JS}(P_\tau)^{1/2}$  will have an absolute minimum at  $C = 0$ .

Figure 5 depicts  $\delta_K(\alpha, \beta)$  and  $D_{JS}(P_\tau)^{1/2}$  as functions of  $C$ . The salient points are the following.

- The algebraic similarity distance  $\delta_K(\alpha, \beta)$  achieves its highest value (maximum dissimilarity between the time series  $\alpha$  and  $\beta$ ) at weak synchronization ( $C = 0.55$ ), and its lowest values (maximum similarity between  $\alpha$  and  $\beta$ ) at strong synchronization. The transition is monotone and steep.
- On the other hand, the entropic Jensen-Shannon distance  $D_{JS}(P_\tau)^{1/2}$  achieves a local maximum (i.e., a locally high dissimilarity between the probability distributions  $P_\tau$  and  $U$ ) at weak synchronization ( $C = 0.55$ ), and a flat global maximum (i.e., maximum dissimilarity between  $P_\tau$  and  $U$ ) at strong synchronization.

The results for  $\delta_K(\alpha, \beta)$  agree with those obtained in Amigó and Dale<sup>16</sup> using empirical probability distributions

for the Kendall distance and  $L = 4, 5$ , which state that short distances are forbidden in the first case, while long distances are forbidden in the second one. This disparity (also reflected in the transcript order classes, Section VIC) confirms that the nature of the weak and strong synchronization regimes is different.

In sum, both the algebraic distance  $\delta_K(\alpha, \beta)$  and the entropic distance  $D_{JS}(P_\tau)^{1/2}$  are sensitive to the occurrence of synchronization, however,  $\delta_K(\alpha, \beta)$  does so more clearly and distinctively. Actually, judging by the results obtained in the previous numerical simulations,  $\delta_K(\alpha, \beta)$  is the best performer of all transcript-based tools considered in Section VI.

## VII. CONCLUSIONS

This study discusses the role of transcripts in algebraic representations of time series, introducing a novel transcript-based tool for the analysis of coupled time series in the same representation. Remember that the transcript  $T(a, b)$  from an element  $a$  of a finite group  $(\mathcal{G}, \cdot)$  to another group element  $b$ , was defined in Section IV as  $T(a, b) = b \cdot a^{-1} =: T_{a,b}$ .

Regarding the objective (1) in the Introduction (overview of transcripts and their applications), we set the necessary framework in Sections (II)-(IV) and revisited a selection of transcript-based tools in Section V, along with a representative sample of published applications. In particular, we reminded the relationship between transcripts and the Cayley and Kendall distances:  $d_{C,K}(a, b) = \|T_{a,b}\|_{C,K}$  if  $\mathcal{G} = (\text{Sym}(L), *)$ , equation (50). In Section VF we showed that the distances  $d_{C,K}$  can be “transported” to distances  $D_{C,K}^{(\Phi)}$  on any other group  $\mathcal{G}$  via Cayley’s isomorphism  $\Phi: \mathcal{G} \rightarrow \text{Sym}(\mathcal{G})$  (Theorem 5). Furthermore, Cayley’s isomorphism can be im-

plemented using transcripts (Section IV).

When using Cayley’s isomorphism and equation (57) to define the distance  $D_{C,K}^{(\Phi)}$  in a group  $\mathcal{G} \neq \text{Sym}(L)$ , we are encoding the  $|\mathcal{G}|$  elements of  $\mathcal{G}$  as permutations on  $\mathcal{G}$ . According to Cicirello<sup>74</sup>, there are efficient algorithms (such as the bubble-sort algorithm) that compute  $D_C^{(\Phi)}$  in time  $O(|\mathcal{G}|)$ , and  $D_K^{(\Phi)}$  in time  $O(|\mathcal{G}| \log |\mathcal{G}|)$ . Therefore, the embedding of  $\mathcal{G}$  into  $\text{Sym}(\mathcal{G})$  to endow  $\mathcal{G}$  with the distance  $D_{C,K}^{(\Phi)}$  is a computationally competitive method for the low cardinality alphabets used in practice. For example, the calculation of  $(D_K^{(\Phi)}(a_t, b_t))_{1 \leq t \leq N}$  when  $\mathcal{G} = \text{Sym}(6)$  ( $|\mathcal{G}| = 6! = 720$ ),  $N = 10,000$ , and  $\Phi(\mathbf{r})$  is the right translation  $\mathbf{s} \mapsto \mathbf{r} \circ \mathbf{s} = \mathbf{s} * \mathbf{r}$ , took 2.84 seconds using a non-parallelized algorithm running on a laptop computer<sup>16</sup>.

Regarding the objective (2) (benchmarking with numerical simulations), we chose four traditional transcript-based tools (entropy-complexity plane, transcript mutual information, order classes, and Jensen-Shannon distance), as well as the Kendall distance, which has a higher discriminatory power than the Cayley distance due to its larger range (except for  $\text{Sym}(2)$ ); see equations (45)-(46). The numerical simulations consisted of detecting generalized synchronization in the drive-response system (63)-(64) composed of two, non-identical Hénon maps. The best performer turned out to be the novel similarity distance  $\delta_K(\alpha, \beta)$ , which is the mean Kendall distance defined in equation (71).

Precisely, the objective (3) in the Introduction refers to the similarity distance. First of all, we remark its simplicity. As suggested in Section VID, its excellent performance in the numerical simulations is related to the existence of forbidden transcripts (i.e., zero probability transcripts) in the cases of weak and strong synchronization. These results support the idea that the novel similarity distance will also perform well in different contexts, confirming its utility in time series analysis.

In retrospect, the main contributions in the previous sections can be summarized as follows.

- (i): Introduction of the novel similarity distance (71). We found that this transcript-based tool outperforms the others tested in Section VI.
- (ii): Derivation of the right-invariance of  $d_{C,K}$  using transcripts (equations (47)-(48)). In turn, the right-invariance of  $d_{C,K}$  amounts to the Cayley and Kendall distances being norms of transcripts (equation (50)).
- (iii): Transportation of the algebraic distances  $d_{C,K}$  from  $\text{Sym}(L)$  to a general group  $(\mathcal{G}, \cdot)$  via Cayley’s embedding. This approach is practical for the small cardinalities  $|\mathcal{G}|$  used in practice. Moreover, calculating with  $D_{C,K}^{(\Phi)}$  dispenses with the search for minimal descriptions of group elements as products of generators.
- (iv): Verification that the algebraic order in  $\text{Sym}(L)$ , sometimes used as a “dissimilarity” measure in the literature<sup>14</sup>, is actually a distance in strict sense after subtracting one for  $L = 3$  (since it coincides with the Cayley distance); see equation (70).

(v): Interpretation of the similarity distance’s performance in the numerical simulations ( $\mathcal{G} = \text{Sym}(3)$ ) in terms of forbidden transcripts when the system (63)-(64) is in weak or strong generalized synchronization.

(vi): Existence of gaps in the transported distances  $D_{C,K}^{(\Phi)}$ . These gaps must be identified to avoid misinterpreting them as a characteristic of the underlying dynamics. This can be done by calculating the row  $(D_{C,K}^{(\Phi)}(e, c))_{c \in \mathcal{G}}$  of the distance matrix, or using independent white noises for the source and target time series.

Of the above contributions, which include both theoretical and practical matters, we may conclude that transcripts are useful tools in time series analysis. In particular, the similarity distance results in our numerical simulations are very promising.

The concept of transcript, as defined in equation (10), can be generalized in different ways while preserving its instrumental properties but, so far, no such generalizations have proven to be as handy and practical as the original concept. This suggests that future research in the theory and practice of algebraic representations should focus on the development of new tools and applications. Actually, the applications of algebraic distances in the analysis of time series is the topic of current research. In this regard, we hope that this paper will pave the way for new algebra-based tools and applications in group-valued time series analysis.

## ACKNOWLEDGMENTS

We are very grateful to our reviewers for their constructive criticism, which contributed decisively to improving the original manuscript.

## DATA AVAILABILITY STATEMENT

The data that support the findings of this study are available from the corresponding author upon reasonable request.

## REFERENCES

- <sup>1</sup>H. Kantz and T. Schreiber, *Nonlinear Time Series Analysis*. Cambridge University Press, Cambridge, 1997.
- <sup>2</sup>Y. Hirata and J.M. Amigó, “A review of symbolic dynamics and symbolic reconstruction of dynamical systems,” *Chaos* **33**, 052101 (2023).
- <sup>3</sup>J. Zhang and M. Small, “Complex network from pseudoperiodic time series: Topology versus dynamics,” *Phys. Rev. Lett.* **96**, 238701 (2006).
- <sup>4</sup>M. Small, “Complex networks from time series: Capturing dynamics,” in 2013 IEEE International Symposium on Circuits and Systems (ISCAS) (IEEE, 2013), pp. 2509–2512.
- <sup>5</sup>Y. Zou, R.V. Donner, N. Marwan, J.F. Donges, and J. Kurths, “Complex network approaches to nonlinear time series analysis,” *Physics Reports* **787**, 1–97 (2019).
- <sup>6</sup>P.Y. Lum, G. Singh, A. Lehman, T. Ishkanov, M. Vejdemo-Johansson, M. Alagappan, J. Carlsson, and G. Carlsson, “Extracting insights from the shape of complex data using topology,” *Scientific Reports* **3**, 1236 (2013).

- <sup>7</sup>J.A. Perea, "Topological time series analysis," *Notices of the American Mathematical Society* **66**, 686-694 (2019).
- <sup>8</sup>T. Haruna, "Complexity of couplings in multivariate time series via ordinal persistent homology," *Chaos* **33**, 043115 (2023).
- <sup>9</sup>J.M. Amigó, R. Monetti, B. Graff, and G. Graff, "Computing algebraic transfer entropy and coupling directions via transcripts," *Chaos* **26**, 113115 (2016).
- <sup>10</sup>C. Bandt and B. Pompe, "Permutation Entropy: A Natural Complexity Measure for Time Series," *Physical Review Letters* **88**, 174102 (2002).
- <sup>11</sup>M. Mohr, F. Wilhelm, M. Hartwig, R. Möller, and K. Keller, *New Approaches in Ordinal Pattern Representations for Multivariate Time Series. Proceedings of the Thirty-Third International Artificial Intelligence Research Society Conference (FLAIRS 2020)*, pp. 124–129, North Miami Beach, Florida, 2020. <https://aaai.org/papers/124-flairs-2020-18417>.
- <sup>12</sup>I.N. Herstein, *Abstract Algebra*, Wiley 1996. ISBN 978-0471368793.
- <sup>13</sup>S. Lang, *Undergraduate Algebra* (3rd edition). Undergraduate Texts in Mathematics, Springer, New York, 2005. ISBN 978-0387220253.
- <sup>14</sup>R. Monetti, W. Bunk, T. Aschenbrenner, and F. Jamitzky, "Characterizing synchronization in time series using information measures extracted from symbolic representations," *Physical Review E* **79**, 046207 (2009).
- <sup>15</sup>J.M. Amigó, R. Monetti, T. Aschenbrenner, and W. Bunk, "Transcripts: An algebraic approach to coupled time series," *Chaos* **22**, 013105 (2012).
- <sup>16</sup>J.M. Amigó and R. Dale, "Permutation-based distances for groups and group-valued time series," *Entropy* **27**, 913 (2025).
- <sup>17</sup>A. Myers and F. A. Khasawneh, "On the automatic parameter selection for permutation entropy," *Chaos* **30**, 033130 (2020).
- <sup>18</sup>C. Bian, C. Qin, Q.D.Y. Ma, and Q. Shen, "Modified Permutation Entropy Analysis of Heartbeat Dynamics," *Physical Review E* **85**, 021906 (2012).
- <sup>19</sup>V.A. Unakafova and K. Keller, "Efficiently measuring complexity on the basis of real-world data," *Entropy* **15**, 4392-4415 (2013).
- <sup>20</sup>A. Schnurr and S. Fischer, "Generalized Ordinal Patterns Allowing for Ties and Their Applications in Hydrology," *Computational Statistics and Data Analysis* **171**, 107472 (2022).
- <sup>21</sup>E. Tan, S. Algar, D. Corrêa, M. Small, T. Stemler, D. Walker, "Selecting embedding delays: An overview of embedding techniques and a new method using persistent homology," *Chaos* **33**, 032101 (2023).
- <sup>22</sup>W. Bunk, J.M. Amigó, T. Aschenbrenner and R. Monetti, "A new perspective on transcripts by means of their matrix representation: Some properties and applications to coupled systems," *European Physical Journal Special Topics* **222**, 363–382 (2013).
- <sup>23</sup>T. Haruna, "Partially ordered permutation complexity of coupled time series," *Physica D* **388**, 40–44 (2019).
- <sup>24</sup>A.M.Y. Rios de Sousa, and J.Hlinka, "Assessing serial dependence in ordinal patterns processes using chi-squared tests with application to EEG data analysis," *Chaos* **32**, 073126 (2022).
- <sup>25</sup>T. Haruna and K. Nakajima, "Permutation complexity via duality between values and orderings," *Physica D* **240**, 1370–1377 (2011).
- <sup>26</sup>K. Keller and H. Laufer, "Symbolic analysis of high dimensional time series," *International Journal of Bifurcation and Chaos* **13**, 2657–2668 (2003).
- <sup>27</sup>U. Parlitz, S. Berg, S. Luther, A. Schirdewan, J.Kurths, and N. Wessel, "Classifying cardiac biosignals using ordinal pattern statistics and symbolic dynamics," *Computers in Biology and Medicine* **42**, 319–327 (2012).
- <sup>28</sup>U. Parlitz, H. Suetani, S. Luther, "Identification of equivalent dynamics using ordinal pattern distribution," *The European Physical Journal Special Topics* **222**, 553–568 (2013).
- <sup>29</sup>J.S. Cánovas, A. Guillamón, and M. del Carmen Ruiz, "Using permutations to detect dependence between time series," *Physica D* **240**, 1199-1204 (2011).
- <sup>30</sup>C.H. Weiß, "Non-parametric tests for serial dependence in time series based on asymptotic implementations of ordinal-pattern statistics," *Chaos* **32**, 093107 (2022).
- <sup>31</sup>C.H. Weiß, M. Ruiz Marín, K. Keller, and M. Matilla-García, "Non-parametric analysis of serial dependence in time series using ordinal patterns," *Comput. Stat. Data Anal.* **168**, 107381 (2022).
- <sup>32</sup>D. Arroyo, G. Álvarez, and J.M. Amigó, "Estimation of control parameters from symbolic sequences: unimodal maps with variable critical point," *Chaos* **19**, 023125 (2009).
- <sup>33</sup>J.B. Fraleigh, *A First Course in Abstract Algebra*. Pearson New International Edition, 2013. ISBN 978-1292024967.
- <sup>34</sup>C. Bandt, "Small order patterns in big time series: A practical guide," *Entropy* **21**, 613 (2019).
- <sup>35</sup>C. Bandt and F. Shiha, "Order patterns in time series," *Journal of Time series* **28**, 646-665 (2007).
- <sup>36</sup>B.P. Kitchens, *Symbolic Dynamics*. Springer Verlag, Berlin, 1998.
- <sup>37</sup>D. Lind and B. Marcus, *Symbolic Dynamics and Coding*. Cambridge University Press, Cambridge, 2003.
- <sup>38</sup>B.L. Hao and W.M. Zheng, *Applied Symbolic Dynamics and Chaos*. World Scientific, Singapore, 1998.
- <sup>39</sup>J. P. Eckmann and D. Ruelle, "Ergodic theory of chaos and strange attractors," *Rev. Mod. Phys.* **57**, 617–656 (1985).
- <sup>40</sup>D.L. Johnson, "Minimal Permutation Representations of Finite Groups," *American Journal of Mathematics* **93**, 857–866 (1971). JSTOR 2373739.
- <sup>41</sup>M.A. Grechkooseeva, "On Minimal Permutation Representations of Classical Simple Groups," *Siberian Mathematical Journal* **44**, 443–462 (2003).
- <sup>42</sup>M. Zani, L. Zunino, O.A. Rosso, and D. Papo, "Permutation entropy and its main biomedical and econophysics applications: A review," *Entropy* **14**, 1553–1577 (2012).
- <sup>43</sup>J.M. Amigó, K. Keller, and V. Unakafova, "Ordinal symbolic analysis and its applications to biomedical recordings," *Philosophical Transactions of the Royal Society A* **373**, 20140091 (2015).
- <sup>44</sup>M. Adams and K. Lehnertz, "Noise robustness of transcript-based estimators for properties of interactions," *Entropy* **27**, 1067 (2025).
- <sup>45</sup>T.M. Cover and J.A. Thomas, *Elements of Information Theory*, 2nd edition. New York, John Wiley & Sons, 2006.
- <sup>46</sup>J.M. Amigó and K. Keller, "Permutation entropy: One concept, two approaches," *European Physical Journal Special Topics* **222**, 263–274 (2013).
- <sup>47</sup>A. Rényi, On measures of entropy and information. In *Proceedings of the 4th Berkeley Symposium on Mathematics, Statistics and Probability*; J. Neyman, Ed.; University of California Press: Berkeley, CA, USA, 1961; pp. 547–561.
- <sup>48</sup>C. Tsallis, "Possible generalization of Boltzmann–Gibbs statistics," *J. Stat. Phys.* **52**, 479–487 (1988).
- <sup>49</sup>P. Pilarczyk, G. Graff, J.M. Amigó, K. Tessmer, K. Narkiewicz, and B. Graff, "Differentiating patients with obstructive sleep apnea from healthy controls based on heart rate-blood pressure coupling quantified by entropy-based indices," *Chaos* **33**, 103140 (2023).
- <sup>50</sup>L. Paninski, "Estimation of entropy and mutual information," *Neural Computation* **15**, 1191–1253 (2003).
- <sup>51</sup>M. Riedl, A. Müller, and N. Wessel, "Practical considerations of permutation entropy," *Eur. Phys. J. Spec. Top.* **222**, 249–262 (2013).
- <sup>52</sup>E.T.C. Chagas, A.C. Frery, J. Gambini, M.M. Lucini, H.S. Ramos, and A.A. Rey, "Statistical properties of the entropy from ordinal patterns," *Chaos* **32**, 113118 (2022).
- <sup>53</sup>J. Lin, "Divergence measures based on the Shannon entropy," *IEEE Trans. Inf. Theory* **37**, 145–151 (1991).
- <sup>54</sup>D. Endres and J. Schindelin, "A new metric for probability distributions," *IEEE Trans. Inf. Theory* **49**, 1858–1860 (2003).
- <sup>55</sup>O. A. Rosso, H. A. Larrondo, M. T. Martín, A. Plastino, and M. A. Fuentes, "Distinguishing noise from chaos," *Phys. Rev. Lett.* **99**, 154102 (2007).
- <sup>56</sup>R. Monetti, J.M. Amigó, T. Aschenbrenner and W. Bunk, "Permutation complexity of interacting dynamical systems," *European Physical Journal Special Topics* **222**, 421–436 (2013).
- <sup>57</sup>R. Monetti, W. Bunk, T. Aschenbrenner, S. Springer, and J.M. Amigó, "Information directionality in coupled time series using transcripts," *Phys. Rev. E* **88**, 022911 (2013).
- <sup>58</sup>M. Staniek and K. Lehnertz, "Symbolic transfer entropy," *Physical Review Letters* **100**, 158101 (2008).
- <sup>59</sup>J.M. Amigó, R. Monetti, N. Tort-Colet, and M.V. Sanchez-Vives, "Infragranular layers lead information flow during slow oscillations according to information directionality indicators," *J. Comp. Neuros.* **39**, 53–62 (2015).
- <sup>60</sup>Y. Hirata, J.M. Amigó, Y. Matsuzaka, R. Yokota, H. Mushiake, and K. Aihara, "Detecting causality by combined use of multiple methods: Climate and brain examples," *PLoS ONE* **11**, e0158572 (2016).
- <sup>61</sup>M. Adams, J.M. Amigó, and K. Lehnertz, "Transcript-based estimators for characterizing interactions," *Chaos* **36**, 013104 (2026).
- <sup>62</sup>K. Sørensen, "Distance measures based on the edit distance for permutation-type representations," *Journal of Heuristics* **13**, 35–47 (2007).
- <sup>63</sup>T. Nguyen, "Improving the Gilbert-Varshamov bound for permutation Codes in the Cayley metric and Kendall  $\tau$ -Metric," arXiv:2404.15126v2

- (2024).
- <sup>64</sup>M.G. Kendall, "A new measure of rank correlation," *Biometrika* **30**, 81-93 (1938).
- <sup>65</sup>Permutohedron. <https://en.wikipedia.org/wiki/Permutohedron>.
- <sup>66</sup>S.J. Schiff, P. So, T. Chang, R.E. Burke, and T. Sauer, "Detecting dynamical interdependence and generalized synchrony through mutual prediction in a neural ensemble," *Physical Review E* **54**, 6708-6724 (1996).
- <sup>67</sup>N.F. Rulkov, M.M. Sushchik, L.S. Tsimring, and H.D.I. Abarbanel, "Generalized synchronization of chaos in directionally coupled chaotic systems," *Physical Review E* **51**, 980-994 (1995).
- <sup>68</sup>M.G. Rosenblum, A.S. Pikovsky, and J. Kurths, "From phase to lag synchronization in coupled chaotic oscillators," *Physical Review Letters* **78**, 4193-4196 (1997).
- <sup>69</sup>A. Pikovsky, M. Rosenblum, and J. Kurths, *Synchronization: A Universal Concept in Nonlinear Sciences*, Cambridge University Press, Cambridge, UK, 2001.
- <sup>70</sup>J.M. Amigó, R. Dale, J.C. King, and K. Lehnertz, "Generalized synchronization in the presence of dynamical noise and its detection via recurrent neural networks," *Chaos* **34**, 123156 (2024).
- <sup>71</sup>S. Berger, A. Kravtsov, G. Schneider, and D. Jordan, "Teaching ordinal patterns to a computer: Efficient encoding algorithms based on the Lehmer code," *Entropy* **21**, 1023 (2019).
- <sup>72</sup>A.A.B. Pessa and H.V. Ribeiro, "ordpy: A Python package for data analysis with permutation entropy and ordinal network methods," *Chaos* **31**, 063110 (2021).
- <sup>73</sup>A. Silbernagel and C.H. Weiß, "The joint asymptotic distribution of entropy and complexity," *Chaos* **36**, 023145 (2026).
- <sup>74</sup>V.A. Cicirello, "Kendall tau sequence distance: Extending Kendall tau from ranks to sequences." arXiv:1905.02752v3, 2019.